# Axion strings are superconducting

### Hajime Fukuda $^{a,b}$ Aneesh V. Manohar $^c$ Hitoshi Murayama $^{a,b,d}$ Ofri Telem $^{a,b}$

- <sup>a</sup> Theoretical Physics Group, Lawrence Berkeley National Laboratory, Berkeley, CA 94720, USA
- <sup>b</sup>Berkeley Center for Theoretical Physics, Department of Physics, University of California, Berkeley, CA 94720, USA
- <sup>c</sup>Department of Physics, University of California at San Diego, 9500 Gilman Drive, La Jolla, CA 92093-0319, USA
- <sup>d</sup>Kavli IPMU (WPI), UTIAS, The University of Tokyo, Kashiwa, Chiba 277-8583, Japan

ABSTRACT: We explore the cosmological consequences of the superconductivity of QCD axion strings. Axion strings can support a sizeable chiral electric current and charge, which alters their early universe dynamics. Shrinking axion string loops can become effectively stable remnants called vortons, supported by the electromagnetic force of the string current. Generically, vortons produced by axion strings overclose the universe, unless there are efficient current leakage processes. Furthermore, if a primordial magnetic field (PMF) exists in the early universe, a large current is induced on axion strings, creating a significant drag force from interactions with the surrounding plasma. As a result, the strings are slowed down, which leads to an orders of magnitude enhancement in the number of strings per Hubble volume. Finally, we study the implications for the QCD axion relic abundance. The QCD axion window is shifted by orders of magnitude in some parts of our parameter space.

$\mathbf{C}$	ontents	
1	Introduction	1
2	Fermion Zero-Modes and Axion String Superconductivity	2
3	Current Dissipation	5
4	Vortons	8
5	Axion Abundance with a Primordial Magnetic Field	15
6	Conclusion and Discussion	32

### 1 Introduction

One of the long standing puzzles in theoretical physics is the tiny value of  $\bar{\theta} < 10^{-10} \ll$  1, usually referred to as the strong CP problem. The strong CP problem cannot be solved anthropically [1]. A possible solution is by the Peccei-Quinn (PQ) mechanism [2, 3], where a broken anomalous chiral U(1) symmetry dynamically sets the  $\theta$  angle to zero [4]. PQ symmetry breaking produces a light pseudo-Goldstone boson called the axion [5, 6]. The axion is also a dark matter (DM) candidate.

If the PQ symmetry is broken during inflation, the axion field is frozen during the inflationary era. Eventually, when the Hubble expansion H becomes smaller than the axion mass  $H \ll m_a$ , the axion behaves like a massive particle, and the initial axion field value determines the relic axion density. Quantum fluctuations of the axion are generated, and the isocurvature fluctuation is generally large. To avoid observational constraints [7], the inflationary Hubble scale  $H_{\rm inf}$  must be as small as  $H_{\rm inf} \lesssim 10^7 \, {\rm GeV}$  [8, 9]. If PQ symmetry breaking occurs after inflation, cosmic axion strings, topological defects associated with U(1)<sub>PQ</sub> symmetry breaking, appear after the symmetry breaking phase transition [10–12]. Axion strings are vortices in which the phase of the scalar field rotates by  $2\pi$  around the string, and are topologically stable because  $\pi_1(U(1)_{\rm PQ}) = \mathbb{Z}$ . The  $U(1)_{\rm PQ}$  symmetry is restored in the string core. The dynamics of axion strings is crucial for understanding the relic axion density. We focus on the latter scenario, where PQ symmetry is broken after inflation, in this paper.

In standard cosmic string cosmology, many axion strings appear after the PQ phase transition [13, 14]. They reconnect with each other, reducing the total length of string. Due to friction caused by interactions with the thermal plasma, the number of strings in the Hubble horizon,  $\xi$ , may be larger than  $\mathcal{O}(1)$  at first [15]. As the universe cools, plasma friction weakens and the string abundance eventually enters a scaling regime, where  $\xi \sim \mathcal{O}(1)$  of strings exist per Hubble volume, over many orders of magnitude in temperature until  $T \gtrsim T_{\rm QCD}$ . The scaling of strings in the early universe has been extensively studied by numerical simulations [16–33]. The scaling behavior is the result of a balance between string length entering the horizon, and string length which is lost by the emission of unstable string loops due to efficient string reconnection.

At  $T \gtrsim T_{\rm QCD}$ , the axion gets a mass from QCD non-perturbative effects. This leads to the formation of domain walls, and each axion string becomes the boundary of  $N_{\rm DW}$  domain walls, where  $N_{\rm DW}$  is the coefficient of the PQ-QCD anomaly. Generically,  $N_{\rm DW} > 1$  leads to stable domain walls overclosing the universe, and so most post-inflationary QCD axion scenarios are KSVZ-like [34, 35] with  $N_{\rm DW} = 1$ . In this case the string-domain wall systems are unstable, and they annihilate into cold axions which form the bulk of the DM relic density.

In this paper, we focus on the KSVZ scenario as an example with  $N_{\rm DW}=1$  and point out an important effect — the axion string is (color) superconducting [36]. While our discussion is completely generic and can be applied to any axion scenario, we use the KSVZ example for a quantitative discussion. The superconductivity of axion strings is widely known in the context of Chern-Simons theory, but overlooked in phenomenological studies. We find that superconductivity predicts a metastable remnant of the axion string, the vorton, as discussed previously in Ref. [37–42]. We also find that in the presence of a primordial magnetic field (PMF), the axion relic abundance is considerably larger than previous expectations.

# 2 Fermion Zero-Modes and Axion String Superconductivity

We review the analysis of superconductivity in the KSVZ axion string. The argument is very general, and applies to other axion models as well. This section also serves to define our notation, and introduce features of the model that will play a role in our analysis.

In addition to the Standard Model (SM) fields, the minimal KSVZ model [34, 35] has two chiral fermions  $\psi_L$  and  $\psi_R$  which transform as 3 under color and are weak SU(2) singlets, and a color-singlet complex scalar  $\Phi$  with the interaction Lagrangian

$$\mathcal{L}_{\text{int}} = -\left[y_{\Phi} \, \Phi \bar{\psi}_L \psi_R + \text{h.c.}\right] - V(\Phi) \,. \tag{2.1}$$

The phase of  $y_{\Phi}$  can be absorbed into  $\Phi$  so that  $y_{\Phi}$  is real. The chiral transformation

$$\Phi \to e^{i\alpha}\Phi,$$
  $\psi_L \to e^{i\alpha}\psi_L,$   $\psi_R \to \psi_R,$  (2.2) {eq:3.2}

is anomalous under QCD,  $\theta \to \theta - \alpha$ , and is the PQ symmetry in this theory. This example has  $N_{\rm DW}=1$ . We assume  $\Phi$  acquires a vacuum expectation value (VEV),  $\langle \Phi \rangle = f_a/\sqrt{2}$  which breaks the PQ symmetry and gives  $\psi$  a mass  $m_{\psi} = y_{\Phi}f_a/\sqrt{2}$ . The phase of  $\Phi$  is the axion,

$$\Phi \to \frac{f_a}{\sqrt{2}} e^{ia/f_a} \,, \tag{2.3}$$

and  $f_a$  is the axion decay constant, and  $a/f_a$  has periodicity  $2\pi$ . Since we assume that PQ symmetry breaks after inflation, the KSVZ fermions must decay to standard model particles so as not to dominate the universe. To allow for decays, there have to be interactions between  $\psi$  and SM particles. For example, we can assume that  $\psi$  has Yukawa couplings via the Higgs field H to the SM quark doublet  $Q_L$ ,  $(\tilde{H}_i = \epsilon_{ij} H^{\dagger j})$ 

$$\mathcal{L} = -y\,\overline{Q}_L^i\psi_R H_i + \mathrm{h.c.}$$
 or  $\mathcal{L} = -y\,\overline{Q}_L^i\psi_R \widetilde{H}_i + \mathrm{h.c.}$  (2.4) {eq:psiDecayO

depending on whether  $\psi$  has weak hypercharge Y = -1/3 or Y = 2/3, i.e. the quantum numbers of  $b_R$  or  $t_R$ . These interactions preserve the PQ symmetry Eq. (2.2). Note that because the gauge group of the standard model particles is actually limited to  $G_{\rm SM} \equiv {\rm SU}(3) \times {\rm SU}(2) \times {\rm U}(1) / \mathbb{Z}_6$ ,  $\psi$  must have  $Y = 2/3 \mod 1$ , so that it transforms within  $G_{\rm SM}$  and can decay to the standard model particles. The above two examples are the simplest choices that allow for direct Yukawa couplings without need for additional particles.

The axion string is a topological defect around which the axion, the phase of  $\phi$ , winds by  $2\pi$ . An infinitely straight axion string in the z-direction has the form

$$\Phi(\mathbf{x},t) = \frac{1}{\sqrt{2}} f_a h(r_\perp) e^{i\theta}$$
(2.5) {eq:4}

where  $r_{\perp} = \sqrt{x^2 + y^2}$  is the transverse distance from the string, and  $\theta = \tan^{-1}(y/x)$  is the azimuthal angle. The radial solution  $h(r_{\perp})$  depends on the axion potential  $V(\Phi)$ , with  $h(r_{\perp}) \to 1$  as  $r_{\perp} \to \infty$ , and h(0) = 0 so that  $\Phi$  is non-singular at the origin.

It is well known that axion strings have a chiral fermion zero-mode [43] whose existence is guaranteed by an index theorem [44]. The transverse size of the fermion zero-mode, which is bound to the string, is of order  $1/m_{\psi}$ . The axion string has a left (downward) moving  $\psi$  zero-mode trapped on the string. Since  $\psi$  carries color and hypercharge, the zero-mode carries color and U(1) current along the string. The 1+1

dimensional theory of the fermion zero-mode on the string is a chiral theory, and so it has a U(1) gauge anomaly. Below the electroweak phase transition, we will simply consider the 1+1D gauge anomaly of  $U(1)_{\rm EM}$ ,

$$\partial_{\mu}j_{\text{zero-mode}}^{\mu} = -\frac{N_c e_{\psi}^2}{2\pi} E_z. \qquad (2.6) \quad \{\text{eq:23}\}$$

where  $N_c = 3$ ,  $e_{\psi}$  is the electric charge of  $\psi$  multiplied by e, and  $E_z$  is the electric field at the string core in the z direction, leading to a violation of current conservation on the string. Above the electroweak phase transition, one should instead use the analogous equation for hypercharge. The original 3 + 1 dimensional theory is anomaly free, and has conserved current. The resolution of this paradox by Callan and Harvey [36] is that there is a Goldstone-Wilczek current [45]

$$J_{\text{GW}}^{\mu} = \frac{N_c e_{\psi}^2}{8\pi^2 f_c} \epsilon_{\mu\nu\rho\sigma} \partial^{\nu} a F^{\rho\sigma}$$
 (2.7) {eq:london2}

in the bulk, leading to charge inflow onto the string exactly equal to Eq. (2.6). This current is deposited on the string in the form of massless fermion zero-modes. This mechanism is referred to as anomaly inflow.

We have started from an explicit UV model to see the chiral anomaly on the string. Actually, the anomaly is determined solely by the IR Lagrangian. Let us derive the anomaly flow from the coupling between the axion a and gauge fields. Away from the string core, the fermion  $\psi$  is massive and can be integrated out to give a low-energy Lagrangian for the interaction of the axion with the electromagnetic field

$$L_a = \frac{1}{2} (\partial_{\mu} a)^2 - \frac{1}{4} F_{\mu\nu} F^{\mu\nu} + \frac{N_c e_{\psi}^2}{16\pi^2} \frac{a}{f_a} F^{\mu\nu} \widetilde{F}_{\mu\nu} , \qquad (2.8) \quad \{eq: 24\}$$

with  $\epsilon_{0123} = +1^{1}$  and

$$\widetilde{F}_{\mu\nu} = \frac{1}{2} \epsilon_{\mu\nu\alpha\beta} F^{\alpha\beta} \,. \tag{2.9}$$

Here, we omit the color gauge field for simplicity. The electromagnetic current from the axion coupling is

$$J_a^{\mu} = -\frac{\delta S_a}{\delta A_{\mu}} = -\frac{N_c e_{\psi}^2}{4\pi^2} \widetilde{F}^{\mu\nu} \partial_{\nu} \frac{a}{f_a}, \qquad (2.10) \quad \{\text{eq:CSCurrent}\}$$

which is the same as the Goldstone-Wilczek current Eq. (2.7). The divergence of  $J_a^{\mu}$  is

$$\partial_{\mu}J_{a}^{\mu} = -\frac{N_{c}e_{\psi}^{2}}{4\pi^{2}}\tilde{F}^{\mu\nu} \partial_{\mu}\partial_{\nu}\frac{a}{f_{a}}.$$
(2.11)

<sup>&</sup>lt;sup>1</sup>We use the opposite sign convention as Ref. [46].

The axion field has a winding number around the origin, leading to [36, 47, 48]

$$(\partial_x \partial_y - \partial_y \partial_x) \frac{a}{f_a} = 2\pi \delta^{(2)}(\mathbf{x}_\perp), \qquad (2.12) \quad \{eq: 26\}$$

so that

$$\partial_{\mu} J_{a}^{\mu} = -\frac{N_{c} e_{\psi}^{2}}{2\pi} \widetilde{F}^{xy} \delta^{(2)}(\mathbf{x}_{\perp}) = \frac{N_{c} e_{\psi}^{2}}{2\pi} E_{z} \delta^{(2)}(\mathbf{x}_{\perp}), \qquad (2.13) \quad \{\text{eq:27}\}$$

and is exactly canceled by the zero-mode current divergence Eq. (2.6). The theory on the string must produce the same anomaly with the opposite sign to cancel the divergence of this current regardless of the UV theory.

As is expected from the discussion of the UV model, the current operator is light-like [46, 49];

$$\rho = -I,$$
 (2.14) {eq:ChiralCha

where  $\rho$  is the charge density and I is the current. The minus sign is because the zero-mode is left-moving. Then

$$\partial_{\mu}J^{\mu} = \partial_{t}\rho + \partial_{z}I = -\partial_{t}I - \partial_{z}I. \tag{2.15}$$

If the system is placed in a background electric field that is z-independent, I does not depend on z, and

$$\partial_{\mu}J^{\mu} = -\partial_{t}I = -\frac{N_{c}e_{\psi}^{2}}{2\pi}E_{z}, \qquad (2.16) \quad \{eq: LondonEq\}$$

i.e. the current increases linearly with the applied electric field. Thus, there is no resistivity and the axion string is superconducting. The same holds for the color current.

Superconducting strings from fermion zero-modes were discussed in detail by Witten [50]. The paper considers a vector-like UV theory with both up- and down-moving zero modes. We will see that there are some crucial differences from this analysis because of the chiral nature of axion strings. Charge flow and electrodynamics in the presence of chiral axion strings was studied in Refs. [36, 46, 47, 49], and the rotation of the polarization of electromagnetic waves propagating in the string background was studied in Refs. [47, 49, 51, 52].

### 3 Current Dissipation

{sec:leak}

Besides the accumulation of current on the string, current dissipation plays an important role in our analysis. Ref. [50] considered a vector-like theory with zero-modes

moving in both directions along the string. The zero-modes can collide to produce fermion pairs that escape to infinity if the Fermi energy of the zero-modes exceeds  $m_{\psi}$ , the mass of the fermion at infinity. This pair-production process limits the maximum current on the string [50] by  $\varepsilon_F \leq m_{\psi}$ , where  $\varepsilon_F$  is the Fermi energy. This translates into a maximum current  $I \leq e_{\psi} m_{\psi}/(2\pi) \times 2$ , where  $1/(2\pi)$  is the density of states in 1+1 dimension, and 2 is from adding the current charge carriers in both directions.

The axion string has chiral zero-modes, namely both particle and anti-particle are massless and move in the same direction. Therefore they cannot annihilate among themselves and produce massive fermions which escape to infinity; the process is forbidden by energy-momentum conservation. In other words, there is no maximum current. This can also be seen by making a Lorentz transformation for straight strings [53]. For closed string loops, zero-modes moving in opposite directions can interact; however, this is exponentially small in the radius of the loop  $\sim e^{-m_{\psi}R}$ , from the asymptotic form of the zero-mode solution for large  $r_{\perp}$ . Consequently, the only scattering processes with the potential of reducing the current on the string involve either a plasma particle incident on the string or the oscillation modes of the string.

Interaction with the thermal background is similar to photo-ionization of hydrogen, where an incident photon can ionize the bound electron to a continuum state which escapes to infinity. The hydrogen photo-ionization rate depends on the Fourier transform of the ground-state wavefunction, and is suppressed by  $(\omega a_0)^3$  at low frequencies, where  $\omega$  is the incident photon frequency and  $a_0$  is the Bohr radius. In our problem, the zero-modes is localized in two transverse dimensions, so the cross section for ionization is suppressed by  $p_{\perp}^2/m_{\psi}^2$ , the ratio of sizes of the fermion zero-mode and the wavelength of the incident particle.

At very high temperatures, the current can dissipate by thermal particles scattering off the zero mode, and producing an on-shell  $\psi$  particle which can escape to infinity. Let  $T_b = f_a/b$  be the temperature at which this process is no longer effective. The scattering cross section between the energetic particles and the current is of order  $\sigma \sim 1/f_a^2$ , assuming the trapped fermions have energy of order  $f_a$ . Including the Boltzmann suppression factor in the thermal number density  $n \sim T^3 e^{-E/T}$ , the current loss rate is  $\Gamma \sim b^{-3} e^{-b} f_a$ , using  $m_{\psi} \sim f_a$ . Equating this with the Hubble constant gives  $b \sim \ln(M_p/f_a) \sim 20$  for the range of  $f_a$  we are interested in.

At lower temperatures, the current can decay due to interactions with SM particles via the interaction Eq. (2.4), which depends on the Yukawa coupling y. Prototypical

processes leading to current decrease are

$$\begin{split} \bar{Q} \, + \, \psi_{\text{string}}^0 &\rightarrow \, g + h \,, \\ g \, + \, \psi_{\text{string}}^0 &\rightarrow \, Q + h \,, \\ h \, + \, \psi_{\text{string}}^0 &\rightarrow \, Q + g \,, \end{split} \tag{3.1} \quad \{\text{eq:5.2}\}$$

via t- and s-channel Q exchange, where  $\psi_{\text{string}}^0$  is the string zero-mode. The cross-section for these processes, which are related by crossing, is of order

$$\sigma_{\rm scat} \sim \frac{1}{16\pi s} \left| \frac{Ty}{m_{\psi}} g_s \right|^2 = \frac{1}{16\pi s} \left| \frac{\sqrt{2}Ty}{y_{\Phi} f_a} g_s \right|^2 \sim \frac{\alpha_s y^2}{2y_{\Phi}^2 f_a^2} \frac{T}{\varepsilon_F} = \frac{N_c \alpha_s e_{\psi} y^2}{4\pi y_{\Phi}^2 f_a^2} \frac{T}{I} \,. \tag{3.2}$$

The effective coupling of the zero-mode is suppressed by the transverse wavelength of the incoming fermion relative to the size of the string core,  $p_{\perp}/m_{\psi}$  with  $p_{\perp} \sim T$ , times the coupling y from Eq. (2.4). The  $1/(16\pi s)$  factor is a dimensional estimate of the phase space where  $s \sim T \varepsilon_F$  is the center-of-mass energy squared,  $\varepsilon_F$  is the zero-mode Fermi energy and  $m_{\psi} = y_{\Phi} f_a$ , with  $y_{\Phi}$  from Eq. (2.1), and we have used

$$I = \frac{N_c e_{\psi}}{2\pi} \varepsilon_F \tag{3.3} \quad \{eq:I\}$$

for the zero-mode current by filling fermion zero mode states up to the Fermi energy. The resulting rate to ionize a zero-mode is then

$$\Gamma_{\rm scat} = n_{\rm SM} \, \sigma \, v_{\perp \rm rel} \sim \frac{h_{\star} \zeta(3) T^3}{\pi^2} \sigma_{\rm scat}$$
 (3.4) {eq:dest.r}

where we take  $v_{\perp} \sim 1$  because the zero mode is relativistic, and  $h_{\star} = g_B + (3/4)g_F$  is the effective number of degrees of freedom which can interact with the zero-mode. Comparing this rate to the Hubble friction term, we see that the rate Eq. (3.4) is negligible for temperatures  $T < T_{\text{scat}}$  with

$$T_{\text{scat}} = \left(1.2 \times 10^7 \,\text{GeV}\right) \, \frac{1}{y} \, \left(\frac{f_a}{10^{10} \,\text{GeV}}\right) \left(\frac{I/(N_c e_\psi)}{10^{10} \,\text{GeV}}\right)^{1/2} \left(\frac{y_\Phi^2 g_\star^{1/2}}{h_\star}\right)^{1/2}. \tag{3.5}$$

where  $g_{\star} = g_B + (7/8)g_F$  for all particle species. For temperatures lower than  $T_{\text{scat}}$  we can neglect current dissipation by scattering off the thermal background. The last factor in Eq. (3.5) is order unity, and will be neglected.

The zero-mode can also couple to oscillation modes of the string, which we label as  $X^{\mu}$ , the location of the string world-sheet,

$$X^{\mu} + \psi_{\text{string}}^{0} \to \psi^{*} \to QH$$
. (3.6) {eq:5.6}

On the world sheet this process can be described by an effective operator

$$\mathcal{O} = \partial_{\alpha} X^{\mu} (\partial_{\mu} \bar{\psi}^*) \gamma^{\alpha} \psi_{\text{string}}^0 , \qquad (3.7)$$

which respects the translational invariance of  $X^{\mu}$ . Here,  $\alpha$  is a coordinate on the world sheet. Switching to the canonical normalization for  $X^{\mu} = f_a^{-1} \varphi^{\mu}$ ,  $\mathcal{O}$  is a dimension-three operator with an overall  $1/f_a$  suppression. Therefore, the coupling  $X^{\mu} + \psi_{\text{string}}^0 \to \psi^*$  is suppressed by  $1/f_a$ , while the off-shell  $\psi^*$  propagator gives an additional  $1/(y_{\Phi}f_a)$  suppression, so the overall cross section is

$$\sigma_X = \frac{y^2 s^2}{16\pi y_{\Phi}^2 f_a^4} = \frac{y^2 T^2 \varepsilon_F^2}{16\pi y_{\Phi}^2 f_a^4} = \frac{\pi y^2 T^2 I^2}{4N_c^2 e_{\psi}^2 y_{\Phi}^2 f_a^4},\tag{3.8}$$

where  $s^2/(16\pi)$  is a dimensional estimate of the phase space and the squared amplitude, and we have used Eq. (3.3).  $\sigma_X$  is a cross section in 1+1 dimension for  $X^{\mu}$ , and hence is dimensionless. Multiplying by  $T/\pi$  for the average number of  $X^{\mu}$  modes gives the dissipation rate

$$\Gamma_X = \frac{y^2 T^3 I^2}{4N_c^2 e_\psi^2 y_\Phi^2 f_a^4},\tag{3.9}$$

and falls below the Hubble rate  $\Gamma_X < H$  for  $T < T_X$ ,

$$T_X = \left(3.8 \times 10^2 \,\text{GeV}\right) \, \frac{1}{y} \, \left(\frac{f_a}{10^{10} \,\text{GeV}}\right)^4 \left(\frac{10^{10} \,\text{GeV}}{I/(N_c e_\psi)}\right)^2 \left(\frac{y_\Phi^2 g_\star^{1/2}}{h_\star}\right). \tag{3.10} \quad \{\text{eq:5.9}\}$$

The last factor in Eq. (3.10) is order unity, and will be neglected.

The overall leakage rate is given by

$$\Gamma_{\text{leak}} = \Gamma_{\text{scat}} + \Gamma_X,$$
 (3.11) {eq:5.10}

which in practice means whichever rate is the larger one, and so  $T_{\text{leak}}$ , the temperature at which current destruction is relevant is given by

$$T_{\rm leak} \simeq \min\left(\frac{f_a}{b}, T_{\rm scat}, T_X\right)$$
,  $b \sim 20$ , (3.12) {eq:TDest}

using our estimate for b.

#### 4 Vortons

{sec:Vorton}

One interesting consequence of the charge and current on the string is that it slows the shrinkage of string loops. Suppose we start with a string loop with length L and

current I. For  $I \ll f_a$ , the loop shrinks by emitting axions. As discussed in Sec. 3, if current dissipation by the thermal plasma is suppressed, the charge on the string,

$$Q = -IL$$
, (since  $\rho = -I$ ) (4.1) {eq:7.1}

is conserved and constant, in the absence of current leakage processes, discussed in the previous section. As the loop shrinks, the current grows and eventually saturates. This is seen from the total energy of the loop, which is the sum of the tension and the current energy for  $L \gg f_a^{-1}$  and  $I \ll f_a$ . The latter is given

$$E \simeq N_c \frac{\varepsilon_F^2 L}{2\pi} = \frac{2\pi Q^2}{N_c e_{\psi}^2 L}.$$
 (4.2) {eq:7.2}

The total energy is

$$E_{\rm tot}(L) \simeq \mu L + \frac{2\pi Q^2}{N_c e_{tb}^2 L}.$$
 (4.3) {eq:7.3}

where  $\mu \simeq \mathcal{C}f_a^2$  is the tension of the string and

$$C \equiv \pi \log(f_a L). \tag{4.4}$$

Ignoring L dependence of C, the minimum of the energy is given at

$$L \sim L_v \equiv \sqrt{\frac{2\pi}{\mathcal{C}N_c}} \frac{Q}{e_{\psi} f_a} \tag{4.5}$$

or equivalently

$$I \sim I_v \equiv e_\psi \sqrt{\frac{N_c \mathcal{C}}{2\pi}} f_a.$$
 (4.6) {eq:CurrentUp}

Consequently, the mass of the loop at the minimum is given as

$$M_v \simeq \sqrt{\frac{8\pi \mathcal{C}}{N_a}} \frac{Qf_a}{e_{ab}}.$$
 (4.7) {eq:VortonMas}

The loop stops shrinking once the current reaches this value. Such static loops are called *vortons*. Vortons were first predicted for the superconducting cosmic string in Ref. [37] and extensively studied in the '90s [38–42]. Later, it was analytically shown that the loop is stable if the current is chiral [54]. In addition to the trapped current, the vorton also has a cloud of charge carried by the Goldstone-Wilczek current of the gauge

field around the vorton [46]. However, this contribution is suppressed by  $N_c e_{\psi}^2/4\pi^2$ , and we ignore it for simplicity.

Vortons decay via tunneling or by scattering with the thermal plasma, by the same mechanisms as the dissipation of current discussed in Sec. 3. The tunneling decay rate is of order  $\sim e^{-m_{\psi}L_{v}}$  and is negligible for  $L_{v} \gg m_{\psi}^{-1}$ , which is equivalent to

$$Q \gg \sqrt{\frac{2 N_c C}{2\pi}} \frac{e_{\psi}}{y_{\Phi}}. \tag{4.8}$$

Scattering off the thermal background leads to the dissipation rate

$$\dot{I} = -\Gamma_{\text{leak}} I \tag{4.9}$$

with  $\Gamma_{\text{leak}}$  given in Eq. (3.11). This is because the rate Eq. (3.11) is the rate to ionize a single zero-mode state. The total ionization rate is given by multiplying by  $N_0$ , the zero-mode occupation number, and the current loss rate is thus given by multiplying by  $e_{\psi}N_0$ . On the other hand,  $I = e_{\psi}N_0$ , leading to Eq. (4.9). Consequently, for a string loop with large enough charge, the vorton starts to form at  $T_{\text{leak}}$ .

Let us now estimate the vorton abundance due to the thermal fluctuation. The current on the string is induced by the electric field  $E_z \approx T^2$  over the coherence time 1/T, and Eq. (2.16) gives

$$|I| \sim N_c \, e_\psi \, \frac{T}{2\pi} \,,$$
 (4.10) {eq:ThermalCu

at a temperature T. I fluctuates over a thermal coherence scale  $T^{-1}$ , and can have either sign. While fluctuations result in non-zero charges on the strings, global charge conservation is maintained via the Goldstone-Wilczek current. The local charge density is  $\rho = -I$ . Thus the total charge on a string loop of initial length L is

$$Q(L) = \frac{N_c \, e_\psi \, \sqrt{L \, T}}{2\pi} \simeq 1.2 \times 10^3 \, e_\psi \, \left(\frac{g_\star}{106.75}\right)^{-\frac{1}{4}} \left(\frac{T}{10^8 \, \text{GeV}}\right)^{-\frac{1}{2}} \left(\frac{\xi}{10^6}\right)^{-\frac{1}{4}}, (4.11)$$

taking the r.m.s. average over LT independent segments. In the last equation,  $L = \xi^{-1/2}H^{-1}$  is assumed, where  $\xi$  denote the number of the string per Hubble volume. Here, since the charge on the string moves in the same direction, the Goldstone-Wilczek current is assumed to average the charge to the r.m.s. value. This satisfies Eq. (4.8) and the vorton is indeed formed in the early universe after  $T_{\text{leak}}$ . The vorton size and

mass are then

$$L_v = \sqrt{\frac{\mathcal{C}N_c}{2\pi}} \frac{\sqrt{TL}}{e_{\psi} f_a} \simeq 1.0 \times 10^3 f_a^{-1} \left(\frac{g_{\star}}{106.75}\right)^{-\frac{1}{4}} \left(\frac{T}{10^8 \,\text{GeV}}\right)^{-\frac{1}{2}} \left(\frac{\xi}{10^6}\right)^{-\frac{1}{4}} \sqrt{\pi/\mathcal{C}}$$
(4.12)

$$M_v = \sqrt{\frac{8\pi\mathcal{C}}{N_c}} \frac{Q(L_{\text{loop}})f_a}{e_{\psi}} \simeq 1.3f_a \left(\frac{106.75}{g_{\star}}\right)^{\frac{1}{4}} \sqrt{\mathcal{C}/\pi} \sqrt{\frac{M_p}{T}} \, \xi^{-\frac{1}{4}}. \tag{4.13}$$

In order to estimate the vorton density, we consider string evolution. The comoving number density of strings (per unit area) is

$$n_{\rm str} = \xi \, R^2(t) \, H^2,$$
 (4.14)

where R(t) is the scale factor of the universe.  $n_{\text{str}}$  would have been conserved if not for the string reconnections. Thus, the total length of the string which forms loops,  $L_{\text{tot}}(t)$ , is proportional to the time derivative of  $n_{\text{str}}$ ;

$$\frac{dL_{\text{loop, tot}}}{dt} = -\left(\frac{1}{RH}\right)^3 \frac{dn_{\text{str}}}{dt}.$$
(4.15)

Within a Hubble time,

$$L_{\text{loop, tot}} \simeq \frac{2\xi}{H} - \frac{\dot{\xi}}{H^2},$$
 (4.16)

where we take R(t) = 1 without any loss of generality. The loops of string eventually ends up as vortons. Thus, the number of the vortons at a given Hubble time is given by the ratio between  $L_{\text{loop, tot}}$  and the typical size of each loop,  $L_{\text{loop}}$ . For a string velocity  $v_s$ ,  $L_{\text{loop}} = v_s H^{-1}$  and the number of the loops is

$$N_{\rm loop} = \frac{L_{\rm loop, \ tot}}{L_{\rm loop}} = 2\xi \, v_s^{-1} - v_s^{-1} \frac{\dot{\xi}}{H} \equiv k \, \xi \, v_s^{-1}, \tag{4.17} \quad \{\rm eq: Vorton Number 100 \ keV \ column 1000 \ keV \ column 100 \ keV \ column 1000 \ keV \ column 100 \ keV \ column 1000 \$$

where

$$k \equiv 2 - \frac{\dot{\xi}}{\xi H} \tag{4.18} \quad \{eq:RecEff\}$$

denotes the efficiency of string reconnections.

The vorton energy density at a given Hubble time is  $\rho_v \simeq E_v N_{\text{loop}} H^3$ . In order to compare it with the dark matter number density, it is convenient to normalize it by the entropy density s:

$$\frac{\rho_v}{s} \simeq 1.2 \left(\frac{g_\star}{106.75}\right)^{\frac{1}{4}} \sqrt{C/\pi} \, k \, \xi^{\frac{3}{4}} \, v_s^{-1} \left(\frac{T}{M_p}\right)^{\frac{5}{2}} f_a.$$
 (4.19) {eq:VortonAbu

In the above estimation, assumed that the vorton does not annihilates after it forms. This may be a reasonable assumption for particles, but since the size of the loop is macroscopic at the beginning, there may be some annihilation with other vortons. The opposite limit from no annihilation is to assume that the vorton annihilates efficiently, and only the net current asymmetry of the initial vorton distribution survives. In this case, we can simply replace  $N_{\text{loop}} \to \sqrt{N_{\text{loop}}}$ , obtaining the same equation as Eq. (4.19) with  $k \, \xi^{3/4} \, v_s^{-1} \to \sqrt{k} \, \xi^{1/4} \, v_s^{-1/2}$ . Note that in the above discussion, we have focused on the electromagnetic current, but the same dynamics holds for the color current on the axion string as well. A similar analysis of the color current gives the same order-of-magnitude estimate of the vorton abundance.

Finally, we estimate the values of  $\xi$  and  $v_s$ . In the early universe, the friction force due to scattering with plasma particle decelerates the string and  $\xi > 1$  in general [55, 56]. The scattering cross section between the string and thermal particles with a non-zero Peccei-Quinn charge can be as large as allowed by unitarity,  $\lambda \sim 1/T$  [15]. In the KSVZ scenario, such PQ charged particles are absent in the thermal bath. The axion may exist in the universe, but the scattering cross section between the axion and the string is expected to be geometrical. This is an analogue of the scattering between the magnetic monopole and the photon as the magnetic dual of the axion couples to the string. However, since the string supports the (color) current, a (color) magnetic fields winding the string play a role of an effective thickness of the string. This results a scattering rate as large as the unitarity bound. Ref. [57–59] estimate the cross section as

$$\lambda \sim \frac{I}{\sqrt{\rho}},$$
 (4.20) {eq:MagRad}

where  $\rho$  is the energy density of the thermal plasma. This roughly corresponds to the radius where the pressure between the thermal plasma and the magnetic field induced by the current balances. According to the standard picture [60],  $\xi$  and  $v_s$  are determined in the following way. First, the frictional force per unit length of string is

$$F_{\rm fric} \simeq \langle \lambda v_{\rm rel} n q \rangle \sim T^2 I v_s,$$
 (4.21) {eq:FricForce

where  $\langle \rangle$  is the thermal average for the scattering particles,  $v_{\rm rel}$  is the relative velocity between the particles and the string, n is the number density of the scattering particles and q is the momentum transfer. The typical time scale due to friction is the relaxation time of the string momentum,

$$\tau_{\rm fric} = \frac{\mu v_s}{F_{\rm fric}} \simeq \frac{\mu}{T^2 I}. \tag{4.22}$$

For a typical string distance scale  $L \sim \xi^{-1/2} H^{-1}$ , the force on the string per unit length is from the string curvature

$$F_{\rm str} \simeq \frac{\mu}{L}$$
. (4.23) {eq:StrForce}

The string accelerates for a time  $\sim \tau_{\rm fric}$  and the string velocity is thus limited to

$$v_s \simeq \frac{F_{\rm str}}{\mu} \tau_{\rm fric} \simeq \frac{\mu}{LT^2I}.$$
 (4.24) {eq:StrVelFri

On the other hand,  $\xi$  is also given as  $L \simeq v_{\rm s} H^{-1}$  if we assume the reconnection process occurs, so that  $\dot{n}_{\rm str} \neq 0$ . Then,

$$v_s \simeq \xi^{-\frac{1}{2}}, \qquad \qquad \xi \simeq \frac{T^2 I}{\mu H}, \qquad \qquad (4.25) \quad \{ {\tt eq:xiThermFr} \}$$

which justify the assumption. Note that since  $v_s < 1$ ,  $\xi$  stops decreasing when it reaches a value of order one. For simplicity, we thus assume the number of the string per Hubble horizon is max  $(\xi, 1)$ . With Eq. (4.19), we see  $\rho_v/s \sim T^{15/4}$ . Thus, the temperature  $T_v$  when most vortons form is  $T_v = T_{\text{leak}}$ . In the above estimation, we assume the number of the string just after the PQ phase transition at  $T_{\text{PQ}}$ , where we assume  $T_{\text{PQ}} = f_a$ , is more than  $\xi(T_{\text{PQ}})$  so that the number of the string is monotonically decreasing after the phase transition, which is a reasonable assumption [14].

Now, we compare the vorton abundance with observational constraints. Ref. [42] finds that the only constraint on vortons is that they do not dominate the energy density of the universe (although further study may be needed; see the discussion in the end of this section). We thus plot the vorton abundance normalized by the dark matter density in terms of  $T_v$  in Fig. 1. As we have discussed, we show two estimations, assuming no annihilation or efficient annihilation of vortons, as a solid and dashed line, respectively. As the universe gets cold and  $\xi$  decreases to  $\xi \sim \mathcal{O}(1)$ , the two estimates are expected to coincide since the number vortons in the Hubble horizon is  $\xi \sim \mathcal{O}(1)$ . Indeed, one can see that after the kink in the plot, at which temperature  $\xi$  reaches  $\mathcal{O}(1)$ , the solid and dashed line go together. From the figure, we find the vorton abundance is larger than the dark matter abundance if the current leakage process is not efficient for both estimates. In other words, we conclude that the current leakage process must be efficient.

Note that our analysis of vortons is different from previous work [38–42] in several respects. As far as we can tell, our work is the first to show that vortons are inevitably generated by axion strings. Secondly, our estimate for the overall charge per vorton differs from previous analyses [42]. The underlying reason for our different estimate is that

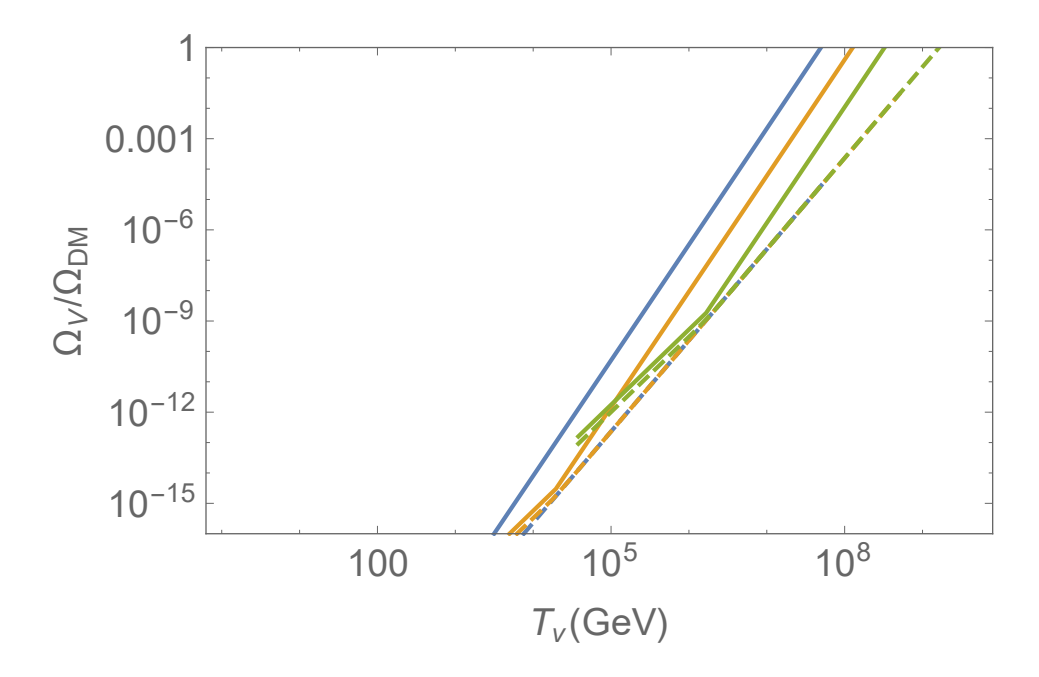


Figure 1. The relic abundance of the vorton,  $\Omega_v/\Omega_{\rm DM}$ , in terms of the vorton formation temperature  $T_v$ . The blue, orange and green lines corresponds to  $f_a=10^9,10^{10}$ , and  $10^{11}\,{\rm GeV}$ . The solid line assumes vortons never annihilate after being formed. The dashed line assumes vortons efficiently annihilate and only the asymmetric component remains. The blue dashed line is overlapped by the orange dashed line. See the text.

{fig:noPMFVor

the Goldstone-Wilczek in the bulk serves to average the current and the charge over the string loop, leading to an overall charge of  $Q \propto \sqrt{TL}$  instead of  $Q \propto TL$ . Consequently, our analysis results in smaller vorton abundances. Finally, though previous analyses concluded that the chiral current on the vortons is completely conserved, we explore several scattering processes that lead to current leakage from the string. When current leakage is efficient enough, the vorton abundance is greatly suppressed, and there is no risk of vortons overclosing the universe. In particular, since  $T_{\text{leak}} < f_a/b < f_a$ , the vorton abundance is insensitive to physics at the PQ scale.

After the QCD phase transition, each string loop becomes the boundary of a domain wall. As the whole system shrinks, the edge current on the string increases. When the current reaches Eq. (4.6), the shrinking of the loop is halted by the repulsive electromagnetic force generated by the current. Since the wall continues to shrink, the domain wall-string system is twisted and eventually breaks into many vortons. Vortons produced by this process are negligible since the energy is only a tiny fraction of the total energy of the string-domain wall network giving the axion dark matter. Note that

if the size of the vorton is larger than the axion compton wavelength (i.e. the domain wall thickness), the same process happens and the vorton breaks into many small vortons. However, the total energy of the vorton is conserved, since it is proportional to the total charge, which is conserved during this breaking process.

It is worth asking whether the superconductivity alters the domain wall dynamics. A domain wall supports some topological field theory to compensate the anomaly [61], but since the wall is much thicker than  $T^{-1}$ , we expect its dynamics is irrelevant. Note that the electromagnetic structure of the domain wall is especially the same as the (anomalous) Hall effect [62].

The charge of the vorton is gigantic  $\gtrsim 10^3$  as Eq. (4.8) requires. The situation is similar to an atomic nucleus with a very large atomic number. Once the charge exceeds  $1/\alpha \sim 137$ , Schwinger pair production [63] occurs and the charge is screened to be  $Q \lesssim 137$ , although the magnetic flux cannot be screened. Similarly, the quark and gluon cloud neutralize the color charge of the vorton after QCD confinement. The color magnetic flux is Higgsed due to the dual Meissner effect [64, 65]. Thus, the vorton looks like a charged exotic hadron with a large magnetic dipole moment. The detection of such an object is not easy [66]. The vorton is screened by the Earth's crust and underground direct detection experiments cannot detect it. In addition, the vorton is much heavier than  $f_a$  and the number density is low. Thus, searches for exotic hadrons do not place any constraints. Consequently, in this section, we require  $\Omega_v < \Omega_{\rm DM}$  based on Ref. [42] although a more detailed discussion of the constraints on vorton abundance remains to be studied.

Note that our discussion is generic and the vorton is an inevitable consequence of the axion string superconductivity, but if we assume another axion model, for instance the variant axion model [67, 68], where the charge carrier is the standard model Fermion, the vorton abundance is different.

### 5 Axion Abundance with a Primordial Magnetic Field

{sec:PMF}

It is widely believed that the intergalactic magnetic field played a role in the formation of the  $\sim 10\,\mu\mathrm{G}$  galactic magnetic fields observed today, via the galactic dynamo effect [69]. The intergalactic magnetic field (IGMF) is characterized by two parameters, the magnitude of the magnetic field B and the typical coherent length  $\lambda$ . An observational lower bound on the IGMF today is set by the non-observation of secondary photons from the emission of highly collimated gamma rays by blazars. Blazar-produced gamma rays collide with CMB photons, and produce highly boosted electron-positron pairs. These, in turn, produce secondary photons which could in principle be detected, if they are collinear enough with the original gamma rays. However, in the presence of a

large enough IGMF, the electrons and positrons bend and no longer produce collinear secondary photons. Recent non-observations of secondary photon put a lower limit of  $B \gtrsim 3 \times 10^{-16}\,\mathrm{G}$  [70] on the IGMF today for  $\lambda \gtrsim 0.1\,\mathrm{Mpc}$ . For shorter coherence lengths, the lower bound becomes even stronger by the factor  $\sqrt{0.1\,\mathrm{Mpc}/\lambda}$ . Though the exact origin of today's IGMF isn't known, one very attractive possibility is that it originated from a primordial magnetic field (PMF). There is a vast literature exploring the different ways a PMF could have been generated in the early universe, a process referred to as magnetogenesis [71, 72]. The strongest upper bound on the PMF scenario is  $B \lesssim 10^{-11}\,\mathrm{G}$ , obtained from CMB perturbations [73].

In this section, we point out that if a PMF is generated in the early universe, it induces very large currents on axion strings, significantly altering their evolution. As a result, the relic abundance of axions may increase by many orders of magnitude. The vorton abundance also increases. Our estimates are based on a simplified analytic model [74], and so should be taken with a grain of salt until a full simulation is conducted. However, we believe that they capture the right physics, and should be explored further using numerical tools.

For later convenience, we define the comoving magnitude of the magnetic field  $\tilde{B} \equiv BR^2$  and the comoving coherent scale  $\tilde{\lambda} \equiv \lambda R^{-1}$ . The dynamics of the magnetic field in the early universe is governed by its interaction with the highly conducting primordial plasma, and is accurately described by magnetohydrodynamics (MHD). The cosmological evolution of plasma-coupled PMF is a complicated problem that was studied by many authors [71, 75], and we will not describe it in detail. Here we include a simplified discussion, and refer the readers to exhaustive reviews [71, 72] for more details.

The key quantity in our simplified analysis is the Alfvén velocity  $v_A \sim \sqrt{\rho_B/\rho_{\rm tot}} \propto B$  [75], where  $\rho_B$  is the energy density of the magnetic field and  $\rho_{\rm tot}$  is the total energy density of the plasma in the early universe. As the universe evolves, the primordial plasma becomes turbulent at scales smaller than the sound horizon  $v_A \tau$ , where  $\tau$  is conformal time. As a result, B fluctuations with a correlation length smaller than the sound horizon get damped (processed), while those with a longer correlation length remain unprocessed. Thus, assuming the typical coherence scale is initially small enough, the coherence scale at conformal time  $\tau$  is given by  $\lambda = v_A \tau \propto B \tau$ . This simple linear relation between B and  $\lambda$  is maintained as the universe expands.

The evolution of B is determined by the the unprocessed component of the magnetic field and the MHD plasma. Let n denote the spectral index of the unprocessed part of the magnetic field and the plasma;  $\tilde{P}(k) \sim \tilde{k}^{-n}$  for the wavenumber smaller than  $\tilde{\lambda}^{-1}$ , where  $\tilde{P}$  is the comoving power spectrum of the magnetic field and of the MHD plasma and is related to the comoving energy density of the MHD flow  $\tilde{\rho}$  by  $\tilde{\rho} \sim \tilde{P}(\tilde{\lambda}^{-1})\tilde{\lambda}^{-3}$ .

Since  $\tilde{\rho} \sim \tilde{B}^2$  at  $\tilde{\lambda}$ , their conformal time dependence is given as [71]

$$\tau^{-1}\,\tilde{\lambda} \;\sim\; \tilde{B} \;\sim\; \tau^{-\frac{3+n}{5+n}} \equiv \tau^{-\alpha}\,. \tag{5.1} \quad \{\text{eq:eqlab}\}$$

The spectral index n can take several different values depending on the dynamics of magnetogenesis. For simplicity, we focus on a PMF coupled to a compressible plasma, where n = 0, and the helical PMF, whose evolution is equivalent to the case n = -2 [71]:

• Compressible plasma: 
$$n = 0$$
  $\alpha = \frac{3}{5}$ 

• Helical PMF: 
$$n = -2$$
  $\alpha = \frac{1}{3}$ 

Another case we consider, is a PMF generated during inflation which is acausal today. The spectrum for this PMF is expected to be scale invariant,<sup>2</sup> and so the typical coherence scale cannot be defined. However, by a slight abuse notation we define  $\tilde{\lambda} = v_a \tau$ . The evolution of the magnetic field and  $\tilde{\lambda}$  is then described by

• Scale Invariant: 
$$n = -3$$
  $\alpha = 0$ .

We stress that in reality the magnetic field in the inflationary scenario can be correlated on super horizon scales. In the following, whenever we mention the scale invariant magnetic field, we simply take it to be comovingly constant ( $\tilde{B}$ =const.) and coherent over the entire Hubble horizon.

When analyzing the effect of the PMF on axion strings in the early universe, we will make use of the average comoving magnetic field  $\tilde{B}(T)$  as a function of temperature. It is useful to relate this quantity to the intergalactic magnetic field  $B_0$  observed today. Naively, the magnetic field decouples from matter at recombination, and the comoving amplitude of the magnetic field remains roughly constant afterwards. From Eq. (5.1), we can naively estimate

$$\tilde{B}(T) = \tilde{B}_0 \left(\frac{\tau_{\text{rec}}}{\tau}\right)^{\alpha} \sim \tilde{B}_0 \left(\frac{T}{\sqrt{T_{\text{eq}}T_{\text{rec}}}}\right)^{\alpha}, \quad \text{(naive)}$$

where  $T_0$  is the current temperature of the photon and  $T_{\text{rec(eq)}}$  is the temperature recombination (the matter-radiation equality). Indeed, a detailed study [75], including viscosity effects and MHD dynamics post matter-radiation equality results in a similar conclusion for  $T \gtrsim 10 \,\text{MeV}$ ;

$$\tilde{B}(T) \simeq \tilde{B}_0 \left( \frac{1}{2.3 \times 10^{-12}} \cdot \frac{T}{100 \, \mathrm{GeV}} \right)^{\alpha}$$
 (5.2) {eq:PMFearly}

<sup>&</sup>lt;sup>2</sup>Note, however, that building a consistent inflationary PMF model is known to be difficult [76].

In this paper, we use the above formula for the PMF as a function of temperature. Note that the coherence length at each time is automatically determined from the Alfvén velocity once  $\tilde{B}$  is fixed. For  $T > T_{\text{rec}}$  [75],

$$\tilde{\lambda}_B^{\text{mag}} = 1.55 \cdot 10^{-4} \text{ pc } \sqrt{\frac{r(T)}{0.01}} \left(\frac{T}{100 \,\text{GeV}}\right)^{-1},$$
(5.3) {eq:Bearly}

where r(T) is the ratio between the magnetic energy and a power of the entropy density [77],

$$r \equiv \frac{R^{-4}\tilde{B}^2}{10} \frac{1}{s^{4/3}}. (5.4)$$

The ratio r would have been a constant if not for the coupling of the PMF to the primordial plasma.<sup>3</sup> After recombination, the coherence length is frozen as well. In terms of  $\tilde{B}_0 = B_0$ , the coherent length of the PMF is [70, 75, 78]

$$\lambda_0 \simeq 11 \,\mathrm{pc} \left( \frac{B_0}{10^{-13} \,\mathrm{G}} \right). \tag{5.5}$$

Combining this with the lower bound on the IGMF introduced in the beginning of this section, we obtain

$$B_0 \gtrsim 0.4 \times 10^{-13} \,\mathrm{G}.$$
 (5.6)

Thus, we take  $10^{-13}$  G as the reference value of the causal  $(n \neq -3)$  PMF today. For acausal (inflationary) PMF, we take the direct lower bound  $3 \times 10^{-16}$  G, as the PMF is assumed to be coherent on a 0.1 Mpc scale.

Having described in some detail the dynamics of a PMF in the early universe, we turn to consider its effect on the cosmic evolution of QCD axion strings. For each one of the PMF types we consider, we vary the initial magnetic field  $^4$   $B_{\rm mag}$  so that its value today is consistent with observations. Since axion strings are superconducting, their interaction with the PMF yields sizeable electric currents, which, as we shall see, back-react on their evolution.

By Lorentz symmetry, a boosted magnetic field becomes an electric field. When the axion string moving with the velocity  $v_s$  is embedded in the PMF, an electric current develops on the string generated by the effective electric field  $E \sim Bv_s$ . The evolution of the current is governed by the electric field, Hubble expansion and current

<sup>&</sup>lt;sup>3</sup>In Ref [75], the magnetic constant is defined as  $\mu_0 \equiv 4\pi$  to convert from SI units to natural units. The value of  $\mu_0$  is always arbitrary and we define  $\mu_0 \equiv 1$  in this paper.

<sup>&</sup>lt;sup>4</sup>We use the subscript "mag" to denote values at the time of magnetogenesis.

dissipation, we obtain the current evolution equation [79], with the addition of a leakage term

$$\dot{I} + I' = \frac{e_{\psi}^2}{2\pi} v_s B - \beta H I - \Gamma_{\text{leak}} I \tag{5.7} \quad \{\text{eq:Bgrowth}\}$$

where I denotes the derivative with respect to the physical time and I' does the derivative with respect to the spacial coördinate on the string. The first term on the right hand side is a direct consequence of Eq. (2.7), while the second term accounts for the redshift of the current due to Hubble expansion. The factor  $\beta$  encodes the effect of the small scale structure of the string; if the string is infinitely long, the current redshift is as usual,  $\beta = 1$  whereas if the string is very wiggly, Hubble expansion straightens the wiggles first so that  $\beta \sim 0$ . We assume  $\beta \sim 1$  in this paper. The current destruction rate  $\Gamma_{\text{leak}}$  is given by Eq. 3.9 and Eq. 3.4. We assume  $y=y_{\Phi}=1$  in the following calculations. For simplicity, when we deal with this equation, we take an average of I(t,z) over the Hubble time. Given that the string velocity is coherent over the typical inter-string distance,  $L \equiv t/\sqrt{\xi}$ , the averaged current I(t) is suppressed by the root-mean-square suppression,  $\sqrt{\ell_{\rm coh}\tau_{\rm current}}$  with  $\ell_{\rm coh}=\min(\lambda,L)$  and  $\tau_{\rm current}\equiv\min(H^{-1},\Gamma_{\rm leak}^{-1})$ . In writing Eq. (5.7), we implicitly assumed that the main mode of energy loss by the strings is string reconnection, which results is a loss of both string length and charge. However, if some of the energy of the strings is directly radiated into axions without the loss of charge, this could induce an additional blue-shift factor, which enhances the current. This effect has been previously considered in [59, 80]. However, we use the above formula as a conservative estimate.

According to Eq. (5.7), the current at a given Hubble time is roughly

$$I(T) \simeq \frac{e_{\psi}^2}{2\pi} v_s B_{\text{eff}} \tau_{\text{current}} \sim \frac{e_{\psi}^2}{2\pi} v_s \sqrt{\ell \tau_{\text{current}}^{-1} r(T)} T^2 \tau_{\text{current}},$$
 (5.8)

where  $B_{\text{eff}} \equiv B\sqrt{\ell_{\text{coh}}\tau_{\text{current}}}$ . If it were not for friction and  $\ell_{\text{coh}} \sim \tau_{\text{current}}$ ,  $v_s$  would be  $\mathcal{O}(1)$  and  $I \sim \frac{e_{\psi}^2}{2\pi}\sqrt{r(T)}M_p$ , which would be much larger than the thermal fluctuation given in Eq. (4.10). Thus, potentially, the current on the axion string by the PMF may significantly affect the evolution of the string. Of course, the current on the string induces friction, as discussed on Sec. 4. The string velocity is decelerated by the friction force as Eq. (4.24). Thus, in order to estimate the current, we need to follow the evolution of the string including friction and evaluate the velocity.

#### 5.1 String Evolution with the PMF

To estimate the effect of the dominant plasma drag on the cosmic evolution of the axion network, we use the analytic velocity dependent one-scale model (VOS) [74, 81], which averages the time evolution of the string energy and velocity using the Nambu-Goto

{sec:PlasmaFr

action. In terms of the average inter-string distance L and the average string velocity  $v_s$ , the equations are

$$2\frac{dL}{dt} = 2LH(1 + v_s^2) + c_L v_s + v_s^2 L \tau_{\text{fric}}^{-1},$$

$$\frac{dv_s}{dt} = (1 - v_s^2) \left[ \frac{k}{L} - v_s \left( 2H + \tau_{\text{fric}}^{-1} \right) \right].$$
(5.9) {eq:VOF}

In the first equation, the first term on the right hand side is from Hubble expansion. The second term encodes the effect of string loop emission by string reconnection.  $c_L$  is a  $\mathcal{O}(1)$  factor of the loop-chopping efficiency, taken as  $c_L \sim 0.34\,[82]$ , and we assume it remains constant. The third term is from friction due to the current. The friction relaxation timescale,  $\tau_{\text{fric}}$ , is defined in Eq. (4.22) for the thermal current, but the formula holds for a generic current. We have ignored the axion emission term and the L dependency of the tension for simplicity. In the second equation, the first term is from acceleration of the string by its curvature. It depends on the small scale structure of the string, which is encoded in the factor k, where we take k = 1 for simplicity. The second term is deceleration by Hubble expansion and friction.

Since  $\tau_{\rm fric}$  is determined by the current on the string as calculated in Eq. (4.22), we combine Eq. (5.7), assuming the average is taken, and Eq. (5.9) to determine the evolution of our current carrying string network once the evolution of the PMF is given. For the PMF time evolution, we simply assume that the magnetic field instantaneously appears at  $T = T_{\rm init}$  and evolves according to Eq. (5.2) for the causal PMF,  $n \neq -3$ . In the following, we vary  $T_{\rm init}$  from around 10 GeV to  $10^3$  GeV as an example. In this setup, the string evolution experiences four distinct stages: (1) the evolution before the PMF appears (2) a transient stage in which the current grows and the string decelerates (3) the stretching phase (4) the friction dominated regime. We find the string never enters the scaling regime after a PMF appears. Below we introduce these stages, and the key processes that characterize them.

#### 5.1.1 Evolution before the PMF appears

Before the PMF appears, the evolution of the axion string follows the standard evolution [10, 13, 14, 60, 74, 81] with the thermal current on the string. According to the standard picture, the string evolution consists of two phases, the friction dominated regime and the scaling regime.

• Friction dominated regime.

Just after the phase transition, numerous strings appear [13, 14]. They strongly interact with each other and quickly decrease forming loops. The number of

strings immediately stops decreasing after the phase transition , since friction due to the thermal current becomes effective, and the strings stop moving. As a result, the number of the string per Hubble horizon,  $\xi$ , obeys Eq. (4.25). As the temperature of the universe drops, friction becomes weaker and eventually negligible. The Kibble temperature, the temperature when friction becomes negligible, is when  $\tau_{\rm fric} \sim H^{-1}$ . To be explicit, it is

$$T_{
m Kibble} = \sqrt{rac{\pi^2 g_{\star}}{90}} rac{\mu}{M_p} \simeq 140 \mathcal{C} \left(rac{g_{\star}}{106.75}
ight)^{1/2} \left(rac{f_a}{10^{10}\,{
m GeV}}
ight)^2 {
m GeV} \,. \eqn(5.10)$$
 {eq:KibbleTem

#### • Scaling regime.

Below  $T_{\text{Kibble}}$ , the universe is cold enough and friction is negligible. The string velocity becomes  $\mathcal{O}(1)$  constant and only  $\xi = \mathcal{O}(1) = \text{constant}$  strings exist in one Hubble volume due to efficient reconnection. As a result, the ratio between the string and radiation energy is constant. This is the scaling regime of the string. Using the VOS model, one may calculate the typical distance and velocity of the string assuming  $L \propto t, v = \text{constant}$  as

$$L_{\text{scaling}}(t) = \sqrt{k(k+c_L)} t, \qquad v_{\text{scaling}}(t) = \sqrt{\frac{k}{k+c_L}}.$$
 (5.11) {eq:Scaling}

Note that in recent years there has been a growing interest in a potential log-arithmic violation of this scaling law,  $\xi > 1$ , backed by dedicated simulations [27–33, 83, 84] though we do not discuss this further.

#### 5.1.2 Transient stage: current growth and string deceleration

At time  $T_{\rm init}$ , the current growth is "turned on" according to Eq. (5.7). Then the current grows rapidly, and there is large plasma friction on the string. The friction relaxation time  $\tau_{\rm fric}$  is much shorter than the Hubble time leading to string deceleration, which in turn feeds back on the current growth equation via its velocity dependence. We call this the transient stage. The whole process ends in a much shorter period than the Hubble time. Since the VOS equation, Eq. (5.9) assumes time-averaging over scales  $\sim H^{-1}$ , such shorter time scale physics cannot be discussed using the VOS equation. For simplicity, we assume L does not change during the transient stage and solve Eq. (5.7) taking spatial averages for I and  $v_s$ . In Fig. 2 we present the numerical solution of this initial stage. As we can see in the plot, the current I grows rapidly until it reaches a plateau, and the velocity decreases accordingly. Indeed, the transient stage ends very quickly, which justifies our assumption. We can estimate the plateau values of I and v by taking R, H, B,  $\lambda$  and L as constants equal to their values at  $t_{\rm init}$ . The plateau

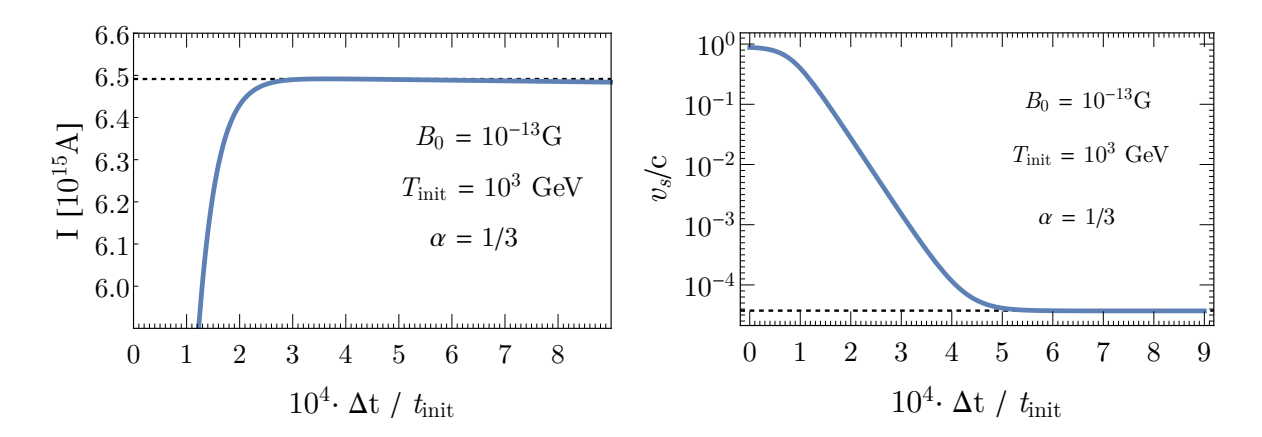


**Figure 2**. Evolution of I and v in the transient stage after  $t_{\text{init}}$ . Left: I(t). Right:  $v_s(t)$ . The dashed lines indicate the plateau values from Eq. 5.12.  $f_a$  is taken to be  $10^{10}$  GeV.

values are then obtained by demanding

$$0 = \frac{dv_s}{dt} = (1 - v_s^2) \left[ \frac{k}{L} - v_s \left( 2H + \tau_{\text{fric}}^{-1} \right) \right],$$

$$0 = \frac{dI}{dt} = \frac{e_{\psi}^2}{2\pi} v_s B - \Gamma_{\text{leak}} I - \beta H I. \qquad (5.12) \quad \{\text{eq:plat}\}$$

{fig:stage1}

We also show these plateau values for  $v_s$  and I in Fig. 2. Numerically, we use these values as initial conditions of the next phase.

#### 5.1.3 Stretching phase

The initial transient phase terminates when  $v_s$  reaches a temporary plateau at  $v_s \ll 1$ . The string can then reconnect to other strings if the distance is smaller than  $v_s H^{-1}$ . However, just after turning on the PMF, the number of the string per Hubble volume is so small that the typical string distance is larger than  $v_s H^{-1}$ . Then, the reconnection does not occur and the number of the string per comoving Hubble volume is constant. This phase is called the stretching regime, since the string is stretched by the Hubble expansion. Let us see how this is realized in the VOS model. Simply ignoring the velocity dependent terms in the L(t) Eq. 5.9, we obtain

$$\frac{dL}{dt} = LH. (5.13) \{eq: VOFstretc$$

Using H = 1/(2t), the solution of the above equation is simple;  $L(t) \sim \sqrt{t}$ . Indeed, the number of strings per comoving Hubble volume,  $(aH)^{-2}/L(t)^2 \sim t^0 = \text{constant}$ .

#### 5.1.4 Plasma friction domination

The stretching regime ends when friction becomes weaker,  $v_s$  increases, and  $v_sH^{-1}$  becomes comparable to the typical string distance. Then reconnection again occurs, but friction is still strong and the whole network evolution again follows the friction dominated regime. The typical string distance and velocity asymptotically follow Eq. (4.25) with  $L = t/\sqrt{\xi}$ . Let us make a rough estimate of  $\xi$ . From Eq. (4.25), we obtain

$$\xi_0 = \sqrt{\frac{90}{\pi^2 g_{\star}}} \frac{IM_p}{\mu}, \qquad v_{s0} = \left(\sqrt{\xi}\right)^{-1} = \left(\frac{\pi^2 g_{\star}}{90}\right)^{1/4} \sqrt{\frac{\mu}{IM_p}},$$
 (5.14)

where the subscript 0 denotes the asymptotic value. On the other hand, the current is

$$I_0 \simeq \frac{e_{\psi}^2}{2\pi} B_{\text{eff}} v_{s0} \tau_{\text{current}}.$$
 (5.15)

Thus, we expect

$$\xi_0 \simeq \left(\frac{e_\psi^2}{2\pi} B_{\text{eff}} \tau_{\text{current}}\right)^{2/3} \left(\sqrt{\frac{90}{\pi^2 q_\star}} \frac{M_p}{\mu}\right)^{2/3} \tag{5.16}$$

as the asymptotic value. For temperatures lower than  $T_{\text{leak}}$ , current dissipation is ineffective and we expect

$$\xi_0 \propto B^{2/3} \ell_{\text{coh}}^{1/3} f_a^{-4/3}.$$
 (5.17)

Note that for all regions of interest,  $\xi \gg 1$  and the axion string *never* enters the scaling regime if the PMF exists, as we numerically show later.

#### 5.1.5 Numerical result

In Fig. 3 we plot the number of strings per Hubble volume  $\xi = (t/L)^2$  and the velocity  $v_s$  as a function of temperature. We take  $f_a = 10^{10} \,\text{GeV}$ ,  $T_{\text{init}} = 10^3 \,\text{GeV}$  and  $B_0 = 3 \cdot 10^{-13} \,\text{G}$  as an example and show the result for  $\alpha = 1/3$  and 3/5. As a comparison, we also show  $\xi$  and  $v_s$  without the PMF.

The figure demonstrates our picture discussed above. First, before  $T_{\rm init}$ , the axion string is at the start of the scaling regime. Without the PMF, the thermal current decays as the temperature drops and the string network enters the scaling regime, although there is an  $\mathcal{O}(1)$  change in  $\xi$ , Eq. (4.25). However, if the PMF appears, it produces a large current on the string and the string is immediately decelerated by plasma friction. For several orders of magnitude in temperature after  $T_{\rm init}$ , the string velocity is too small, and string reconnections are suppressed. Thus, the number of

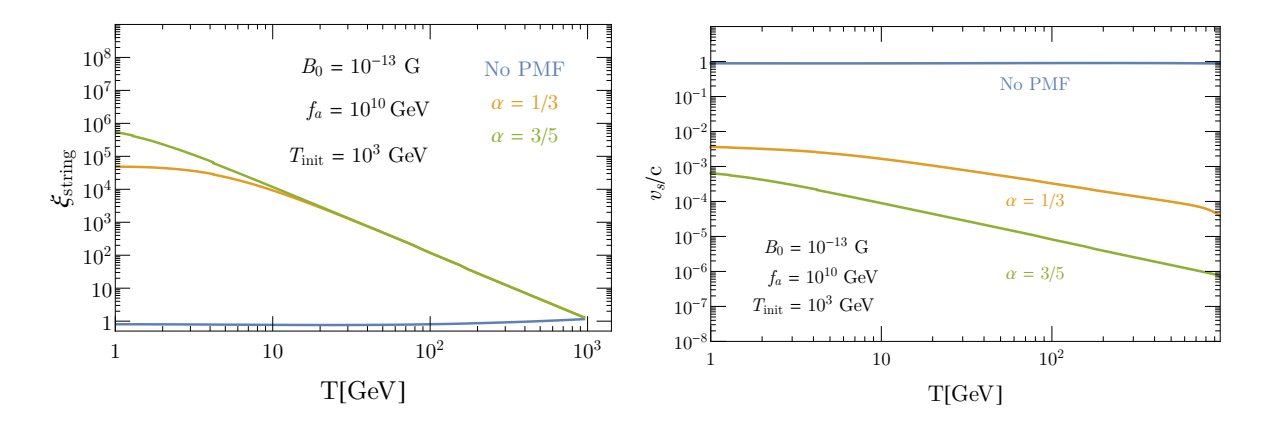


Figure 3. Evolution of current carrying axion strings vs. temperature. Left: Number of strings per Hubble volume  $\xi_{\text{string}}$ . Right: Average string velocity  $v_s$ . The velocity drops immediately when the current is turned on, and then starts growing again due to string curvature.

{fig:xires}

strings per comoving Hubble horizon is conserved and  $\xi$  grows as  $t \sim T^2$ . This regime of string evolution is called the "stretching phase." As the universe gets cold, the PMF and friction force become weaker, allowing the string to accelerates because of its curvature. Eventually, the string network starts to reconnect again and the network goes over to another friction dominated regime. The temperature at which the stretching phase ends depends on the magnitude of the current on the strings, which in turn, depends on the PMF. The larger  $\alpha$  is, the faster the PMF decays. Since we assume the present magnitude of the PMF is the same for both  $\alpha = 1/3$  and 3/5, the PMF at early times is stronger for larger values of  $\alpha$ . Thus, axion strings embedded in a PMF with  $\alpha = 3/5$  spend more time in the stretching regime.

For causal magnetic fields, the temperature of magnetogenesis is bounded from above by the requirement that the PMF does not dominate the expansion of the universe. For that reason, we take  $T_{\rm init}=10^3\,{\rm GeV}$ , which is the relevant upper bound for  $\alpha=3/5$ . For this value of  $T_{\rm init}$ , the  $\alpha=1/3$  case enters the friction dominated regime at around  $T\sim 10\,{\rm GeV}$ , while in the  $\alpha=3/5$  case, the network is approximately still in the stretching regime as late as  $1\,{\rm GeV}$ . In comparison, if  $T_{\rm init}$  is lower than  $10^3\,{\rm GeV}$ , the network is still in the stretching regime at the time of domain wall formation. Eventually, The tension of the domain wall wins over the friction force and the string-domain wall network shrinks and fragments.

### 5.2 Vorton abundance with the primordial magnetic field

As we have discussed in Sec. 4, the current on the string tends to stabilize string loops, leading to vorton formation. When the PMF exists, as we see from the previous sections, large currents may be induced and the vorton abundance may increase. In this section, we estimate the vorton abundance with the PMF.

With the averaged current I from Eq. (5.7), the charge on each vorton is

$$Q_{\text{PMF}} = IL_{\text{loop}} = v_s IH^{-1}.$$
 (5.18) {eq:ChargeVor

The energy of the vorton is then given by

$$E_{v,\text{PMF}} = \sqrt{\frac{8\pi\mathcal{C}}{N_c}} \frac{Q_{\text{PMF}} f_a}{e_{\psi}} \simeq 5.1 \sqrt{\mathcal{C}/\pi} \left(\frac{I}{e_{\psi}}\right) v_s H^{-1} f_a. \tag{5.19}$$

The number of loops in one Hubble volume is the same as Eq. (4.17), and thus assuming no annihilation of vortons (see the discussion after Eq. (4.19)), the energy density of the vorton is

$$\rho_v^{\text{no-ann}} = \sqrt{\frac{8\pi C}{N_c}} \left(\frac{I}{e_{\psi}}\right) k \xi H^2 f_a, \qquad (5.20)$$

whereas assuming efficient annihilation,

$$\rho_v^{\text{eff-ann}} = \sqrt{\frac{8\pi C}{N_c}} \left(\frac{I}{e_{\psi}}\right) \sqrt{k \xi v_s} H^2 f_a, \tag{5.21}$$

although it seems quite unlikely that the charged loop annihilates efficiently in the PMF. Accordingly, the energy density normalized by the entropy density is

$$\frac{\rho_v^{\text{no-ann}}}{s} = \sqrt{\frac{8\pi C}{N_c}} \left(\frac{I}{e_\psi}\right) k\xi \frac{Tf_a}{4M_p^2},\tag{5.22}$$

where  $k\xi$  in the non-log term should be replaced by  $\sqrt{k\xi v_s}$  for the conservative estimate. In the stretching regime, reconnection does not occur so that no loops are emitted. As a result, k=0 and no vorton is created. Vorton are produced just after the stretching regime ends.

#### 5.3 Axion Relic Abundance

Here, we estimate the relic density of axion radiated from axion strings embedded in a PMF. Naively, the increased number of strings per Hubble in our scenario leads to a proportional increase in the number density of radiated axions. However, as reference [33] points out, the actual increase in the axion relic density is roughly proportional to  $\sqrt{\mathcal{C}\,\xi}$ . The reason for that is as follows: The contribution to the relic abundance is biggest when the axion mass starts affecting the dynamics. Since the inter-string distance is  $H^{-1}/\sqrt{\xi}$ , each emitted axion carries a momentum of order  $\sqrt{\xi}H$  and the number of emitted axions is then  $\xi \mu H^{-1}/\sqrt{\xi}H \sim \sqrt{\xi}$ . Assuming the number of axions is conserved, the final relic abundance is proportional to  $\sqrt{\xi}$ . In reality, two corrections should be added to the above estimates. First, since the tension of the axion string is not constant but proportional to  $\mathcal{C}$ , we have to include this factor in our estimate. Secondly, we need to take into account how the axion mass varies with temperature. As a result, Ref. [33] concludes

$$\Omega_{\rm ax} \propto (\mathcal{C}\,\xi)^{\frac{1}{2} + \frac{1}{4 + \gamma}},$$
 (5.23) {eq:marcoest}

where  $\Omega_{\rm ax}$  is the relic abundance of the axion today,  $\gamma$  is the temperature dependence of the axion mass at around  $\lesssim 1 \,{\rm GeV}$ ,  $m_a \propto T^{-\gamma/2}$  and we take  $\gamma \simeq 8$ . The estimate Eq. (5.23) has also been validated by numerical simulations in [33].

We note that the above estimate for the axion relic density relies on an estimate of  $\Gamma_a \sim \rho_s/t$  for the instantaneous axion emission rate, which is valid for strings in the scaling and friction dominated regimes. In our case, though, there is sometimes an exception to that argument, since in the stretching regime reconnection is suppressed and so is axion radiation. To account for this effect, we multiply the estimate  $\sqrt{C\xi}$  by the suppression factor

$$S \equiv \Gamma_a/(\rho_s/t) \,, \tag{5.24}$$

which could be as small as  $10^{-2}$  in the stretching regime.<sup>5</sup>

To calculate  $\Gamma_a$  in our scenario, we evaluate  $\dot{\rho}_s$  for our network evolution, as compared to  $\dot{\rho}_s^{\rm free}$ , an equivalent network of non-interacting strings with the same instantaneous string density at time t,  $\rho_s|_t = \rho_s^{\rm free}|_t$ . The difference between the two terms is the instantaneous energy radiated into loops, and eventually into the axion field [27]:

$$\Gamma_a = \dot{\rho}_s^{\text{free}} - \dot{\rho}_s. \tag{5.25}$$

In Fig. 4 we present the rate  $\Gamma_a$  calculated in this manner, for the network evolution described in Fig. 3. As can be seen in the plot, this rate is suppressed in the stretching regime, but grows to 1 in the friction dominated regime.

Fig. 5 shows contour plots of  $\xi$  at 1 GeV for the causal PMF,  $n \neq -3$ , as a function of the temperature  $T_{\text{init}}$  at which current starts to accumulate, and the magnetic field

<sup>&</sup>lt;sup>5</sup>The VOS equation is for scales around L. The suppression factor is, as we show, much smaller than  $\mathcal{O}(1)$ , which suggests smaller scale physics might be relevant.

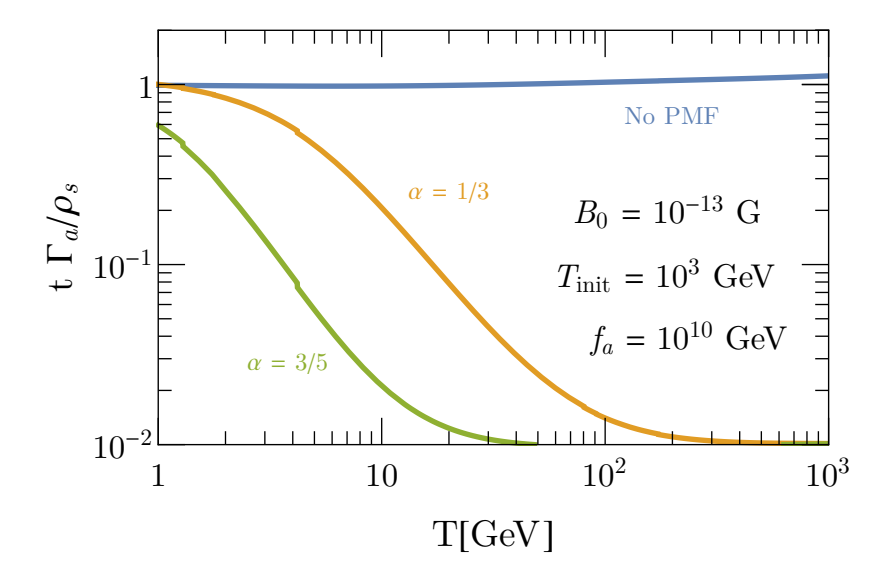


Figure 4. Energy emission rate from axion strings into the axion field, normalized by the approximation  $\rho_s/t$ . In the friction dominated regime, this ratio becomes unity. In the stretching regime, the actual rate is suppressed by up to  $10^{-2}$  due to the low reconnection rate.

{fig:gamma}

 $B_0$  today.  $f_a$  is taken to be  $10^{10}$  GeV here. Note that throughout this section, we assume current leakage is efficient enough, y = 1 in Eq. (3.12). The shaded region is excluded by the magnetic field dominating the universe at magetogenesis [71]. We also confirm that the total energy of the current does not exceed the energy of the magnetic field so that its backreaction on the PMF is negligible.

We present two different contour plots for  $\alpha=1/3$  and  $\alpha=3/5$ . For lower  $T_{\rm init}$ ,  $\xi$  at 1 GeV does not depend on the magnitude of the PMF. This is because the string network is still marginally in the stretching regime at 1 GeV. Indeed,  $\xi$  for  $\alpha=1/3$  and  $\alpha=3/5$  are almost the same. On the other hand, in particular for  $\alpha=1/3$ , if  $T_{\rm init}$  is high enough,  $\xi$  becomes independent of  $T_{\rm init}$ . There, the string network enters the friction dominated regime at 1 GeV and  $\xi$  gets closes to the asymptotic value,  $\xi_0$ .

In Fig. 6, we show  $\xi$  for the inflationary PMF in terms of the magnetic field today. Note that since inflation ends before the Peccei-Quinn phase transition, we may assume  $T_{\rm init} = T_{\rm PQ} = f_a$ . Since the inflationary PMF exists before the PQ symmetry breaking, the network enters the friction dominated regime well above T = 1 GeV and  $\xi$  takes its asymptotic value  $\xi \propto B_0^{4/7}$  (see Eq. (5.16) with  $\ell_{\rm coh} \propto \xi^{-1/2}$ ).

Finally, we show the axion abundance and vorton abundance. In Fig. 7, we show

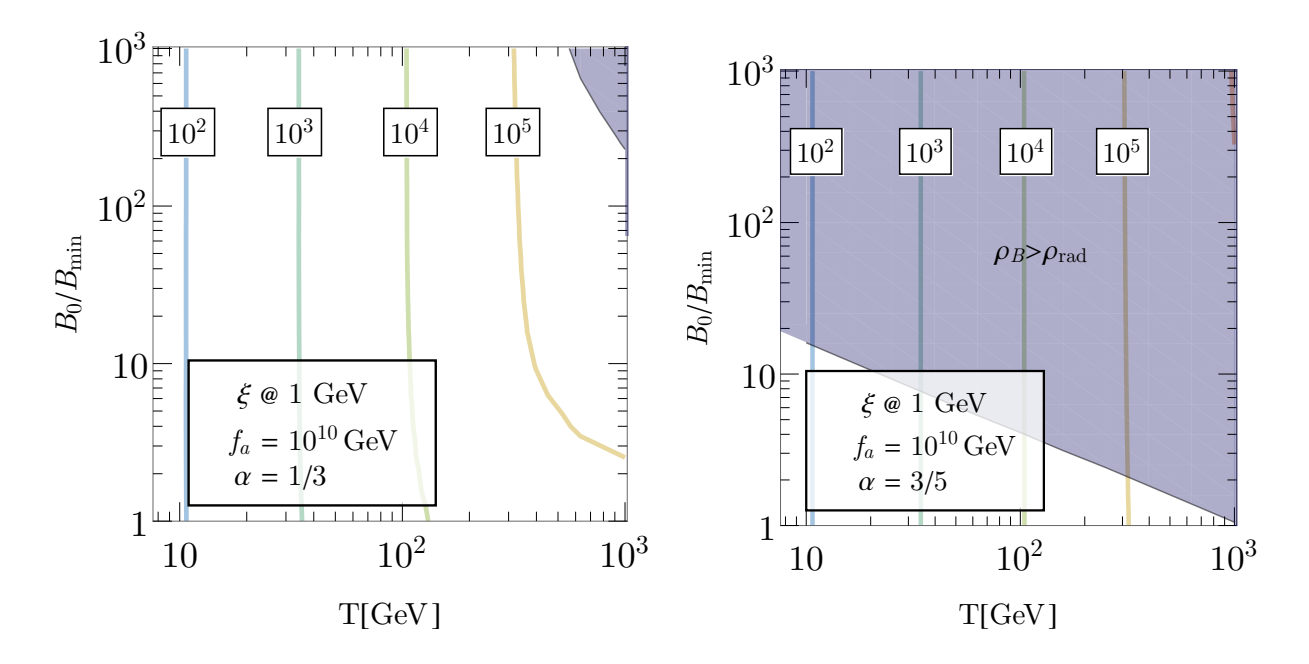
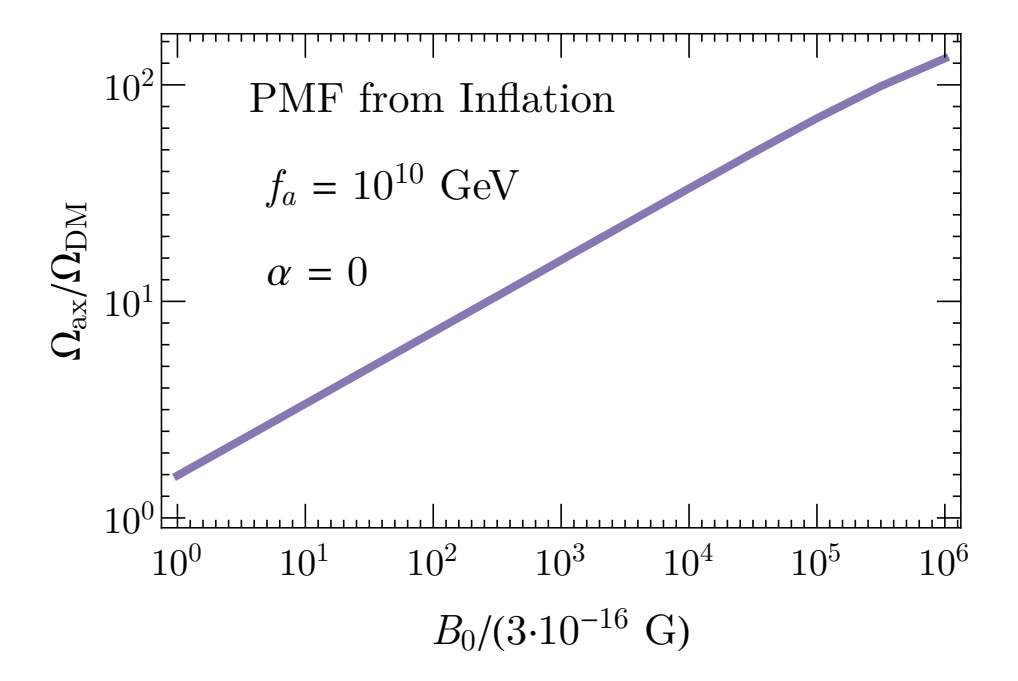


Figure 5.  $\xi$  at T=1 GeV as a function of  $T_{\rm init}$  and  $B_0$  today, scaled by the observed lower bound  $B_{\rm min} \equiv 1 \cdot 10^{-13}$  G. The contours are labelled by the value of  $\xi$  at T=1 GeV.  $f_a$  is taken to be  $10^{10}$  GeV. Left:  $\alpha=1/3$ , Right:  $\alpha=3/5$ .

 $\Omega_{\rm ax}$  determined at 1 GeV for the causal PMF, as a function of the temperature  $T_{\rm init}$ at which current starts to accumulate, and the magnetic field  $B_0$  today. We refer to Ref. [27] for the value of  $\Omega_{\rm ax}$  when  $B_0 = 0$  and scale it by  $\mathcal{S}(\mathcal{C}\xi)^{1/2+1/(4+\gamma)}$ . The parameter region where the vorton abundance exceeds the dark matter abundance is indicated by the green shaded region. Compared with Fig. 5,  $\Omega_{\rm ax}$  is suppressed by the suppression factor. In Fig. 5, we find for lower  $T_{\rm init}$ ,  $\xi$  is independent of  $B_0$ , since the string network is in the stretching phase and the ratio of the comoving Hubble horizon solely determines  $\xi$ . However, the suppression factor is smaller for larger  $B_0$ , since the friction becomes larger and the reconnection occurs less, resulting in smaller  $\mathcal{S}$ . As a result, for fixed  $T_{\rm init} \lesssim 10^2 \, {\rm GeV}$ , where the network is in the stretching phase, the abundance is larger for the smaller  $B_0(>B_{\min})$ . Also, we see  $\xi$  does not depend on  $\alpha$  if the string network is in the stretching regime. However, the PMF is stronger for  $\alpha = 3/5$  scenario and S becomes smaller, as we discuss. Consequently, for fixed  $T_{\rm init} \lesssim 10^2\,{\rm GeV}$ , the axion abundance for  $\alpha = 1/3$  is larger. In Fig. 8, we show  $\Omega_{\rm ax}$ determined at 1 GeV and  $\Omega_v$  for the inflationary PMF in terms of the magnetic field  $B_0$  today (scaled by the observed lower bound  $B_{\rm min} \equiv 3 \cdot 10^{-16} \, \rm G$ ), for  $f_a = 10^{10} \, \rm GeV$ . As we have discussed, for the inflationary PMF, the string network enters the friction



**Figure 6**.  $\xi$  at  $T=1~{\rm GeV}$  as a function of  $B_0$  today, scaled by the observed lower bound  $B_{\rm min}^{\rm inf} \equiv 3 \cdot 10^{-16}~{\rm G}$ , for the inflationary PMF, whose coherent length is assumed to be larger than the current Hubble horizon.  $f_a$  is taken to be  $10^{10}~{\rm GeV}$ .

{fig:scan\_inf

dominated regime at 1 GeV. Thus, the suppression factor is no longer effective and  $\Omega_{\rm ax}$  scales as  $\sim \sqrt{\xi}$ .

To derive the implications for the cosmological bound on  $f_a$ , we now present our results for the axion relic density, while scanning over  $f_a$ . For lower values of  $f_a$ , the string tension is lower and the effect of friction is larger. This makes  $\xi$  larger for these small values of  $f_a$ . On the other hand,  $\Omega_{\rm ax}(\xi=1)$  increases with  $f_a$ , as is well known. The axion abundance is determined by the balancing of these two factors.

In the case where the network is deep in the friction dominated regime by  $T \sim 1 \,\text{GeV}$ , we can use Eq. (5.16) to estimate  $\xi \sim \mu^{-2/3}$  with  $\xi$  dependence of  $\ell_{\text{coh}}$  ignored, and so  $\Omega_{\text{ax}} \sim f_a^{-2/3}$ . On the other hand,  $\Omega_{\text{ax}}(\xi=1) \sim f_a$ . Thus, in total, we expect  $\Omega_{\text{ax}} \sim f_a^{1/3}$  in this limit. In practice the network is either in the stretching regime or on the cusp between the two regimes, and so there is an extra  $f_a$  dependent contribution from the suppression factor  $\mathcal{S}$ .

Our numerical results are shown in Fig. 9. For  $\alpha = 1/3$ , we show  $\Omega_{\rm ax}/\Omega_{\rm DM}$  vs  $f_a$  for 3 different values of  $B_0$ . The string network is not deep in the stretching regime and the suppression factor  $\mathcal{S}|_{1 \text{ GeV}}$  is  $\mathcal{O}(1)$  in the entire parameter space. Thus, as we expect,

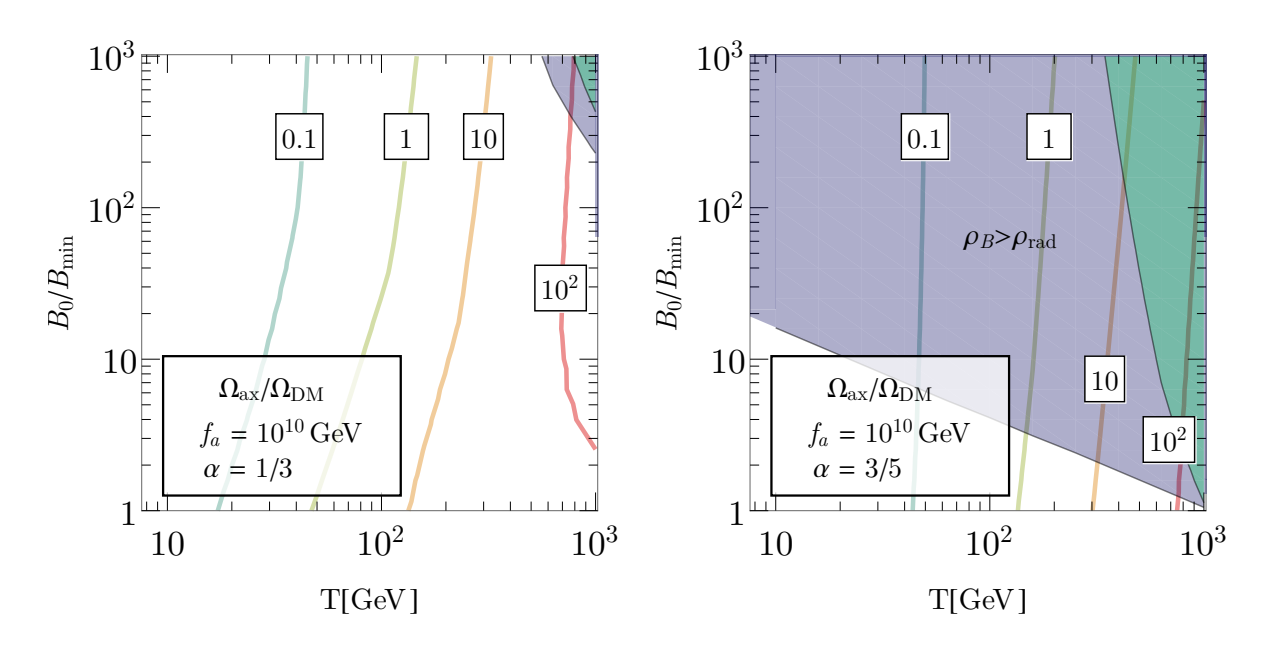


Figure 7.  $\Omega_{\rm ax}/\Omega_{\rm DM}$  as a function of  $T_{\rm init}$  and  $B_0$  today, scaled by the observed lower bound  $B_{\rm min} \equiv 1 \cdot 10^{-13} \,\rm G$ . The contours are labeled by the value of  $\Omega_{\rm ax}/\Omega_{\rm DM}$ .  $f_a$  is taken to be  $10^{10} \,\rm GeV$ . Left:  $\alpha = 1/3$ , Right:  $\alpha = 3/5$ .

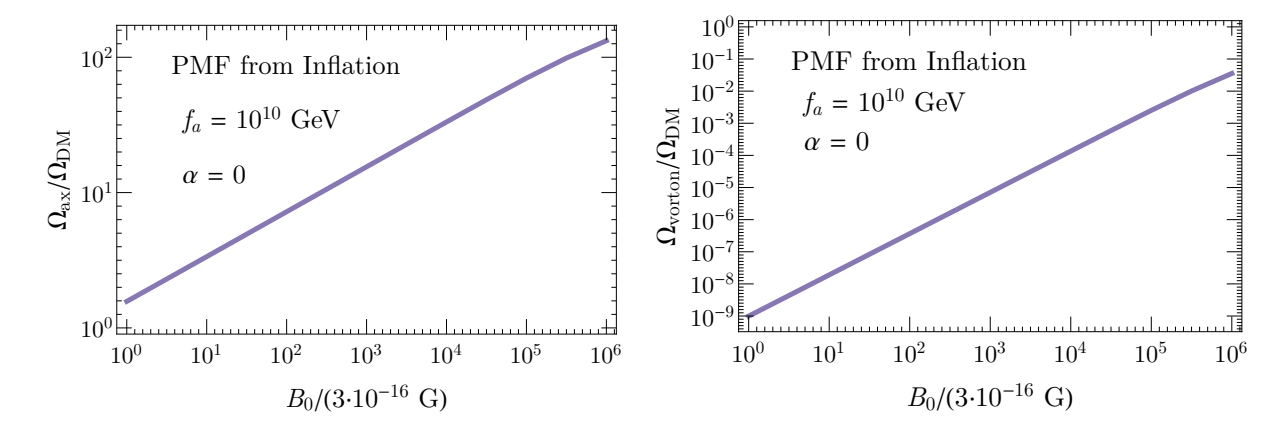


Figure 8. For the inflationary PMF, Left:  $\Omega_{\rm ax}/\Omega_{\rm DM}$ , Right:  $\Omega_{\rm v}/\Omega_{\rm DM}$  as a function of  $B_0$  today, scaled by the observed lower bound  $B_{\rm min} \equiv 3 \cdot 10^{-16} \, {\rm G}$ .  $f_a$  is taken to be  $10^{10} \, {\rm GeV}$ . {fig:XiInf}

 $\Omega_{\rm ax}$  is a mildly increasing function of  $f_a$ , although the exponent is different from 1/3, since the string network is only at the cusp of the friction dominated phase. We find, for example, if  $B_0 = B_{\rm min}$ , the correct relic abundance is given for  $f_a \sim 10^7 \,{\rm GeV}$ . For

 $\alpha = 3/5$ , we show  $\Omega_{\rm ax}/\Omega_{\rm DM}$  in terms of  $f_a$  with changing  $T_{\rm init}$ . In this case, since the magnetic field in the early universe is larger, the whole network may be in the moderate stretching phase and the suppression factor,  $\mathcal{S}$ , may be small.

For smaller  $f_a$ , the eventual axion relic density is affected not only by the PMF, but also by friction from the thermal current on the strings, prior to magnetogenesis. This sets a different initial condition with a higher value of  $\xi$  at the onset of the stretching regime. As a result, the number of strings in the Hubble volume at  $T_{\text{init}}$  is larger for smaller  $f_a$  and the transition from the stretching to the friction dominated phase occurs earlier. Thus,  $\Omega_{\text{ax}}/\Omega_{\text{DM}}$  is no longer monotonically decreasing in  $f_a$ , as can be seen in the right panel of Fig. 9 and in Fig. 10.

We calculated the vorton abundance throughout the parameter space of Fig. 9, but it turn out to be much smaller than  $\Omega_{\rm DM}$ , because the string network is in the stretching phase almost until around 1 GeV and vorton production is suppressed.

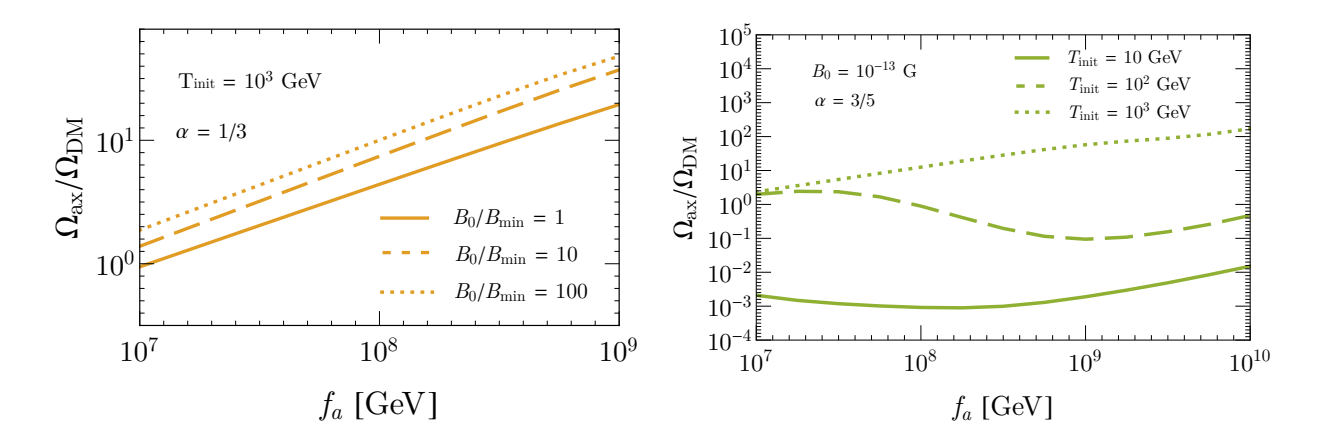


Figure 9.  $\Omega_{\rm ax}/\Omega_{\rm DM}$  as a function of  $f_a$  for a fixed  $T_{\rm init}$  and  $B_0$  today, scaled by the observed lower bound  $B_{\rm min} \equiv 10^{-13} \, \rm G$ , for the causal PMF. Left:  $\alpha = 1/3$  and we change  $B_0$  and see how  $\Omega_{\rm ax}$  behaves for  $T_{\rm init} = 10^3 \, \rm GeV$ . Right:  $\alpha = 3/5$  and we change  $T_{\rm init}$  and see how  $\Omega_{\rm ax}$  behaves for  $B_0 = B_{\rm min}$ .

{fig:OmegaInF

Finally, in Fig. 10 we present a 2D scan of  $\Omega_{\rm ax}/\Omega_{\rm DM}$  as a function of  $f_a$  and  $T_{\rm init}$  for the minimal value  $B_0 = 10^{-13} \,\rm G$  of the magnetic field today. As mentioned before, for  $T_{\rm init} \lesssim 10^2 \,\rm GeV$ , the string network for both  $\alpha = 1/3$  and  $\alpha = 3/5$  is in the stretching regime, and so their value of  $\xi$  is simlar. Even so, the value of  $\Omega_{\rm ax}$  for  $\alpha = 3/5$  is smaller than the one for  $\alpha = 1/3$ , because of its greater friction that leads to a slower string velocity and a smaller value of S.

The axion abundance is also presented for the inflationary scenario in Fig. 11. In

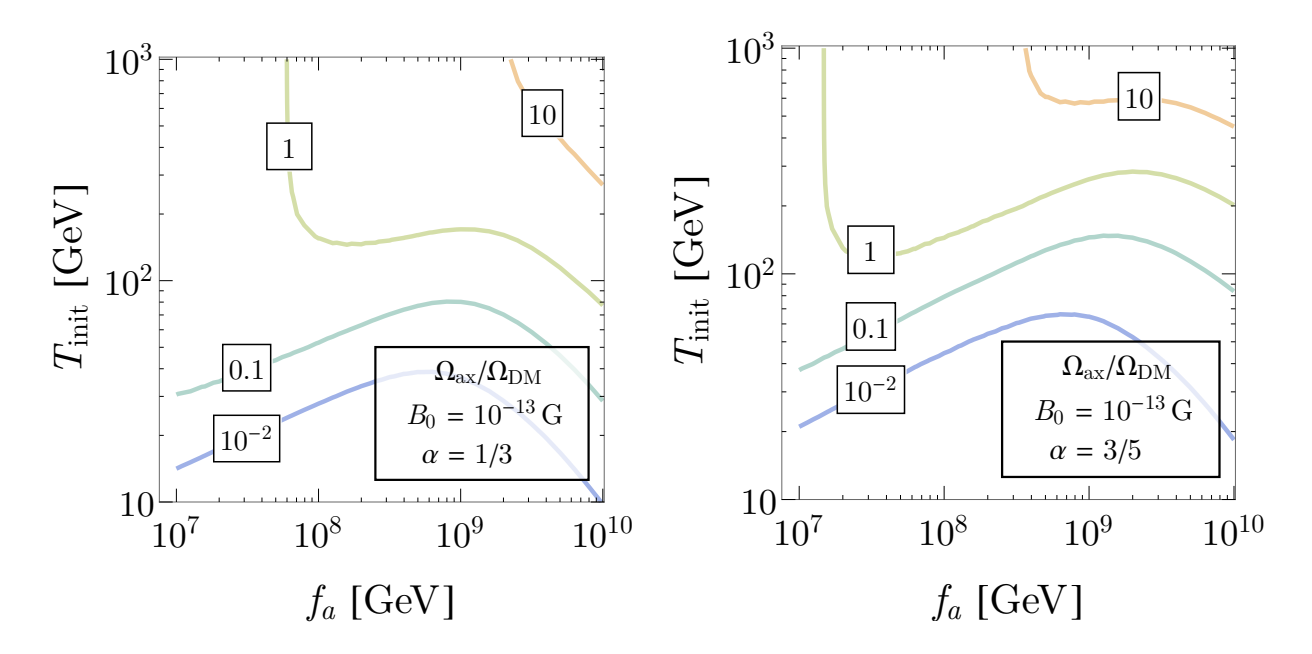


Figure 10. Contour plots of  $\Omega_{\rm ax}/\Omega_{\rm DM}$  as a function of  $f_a$  and  $T_{\rm init}$  for  $B_0=10^{-13}\,{\rm G}$  today. The contours are labelled by the value of  $\Omega_{\rm ax}/\Omega_{\rm DM}$ . Left:  $\alpha=1/3$  Right:  $\alpha=3/5$ 

{fig:OmegaInF

this case, we may assume the asymptotic value of  $\xi$ . As a result,  $\Omega_{\rm ax}/\Omega_{\rm DM}$  scales like HF:  $f_a\sqrt{\xi_0}\sim f_a^{3/7}B^{2/7}$  as one can check in the figure. We also show the vorton abundance. As can be seen from the plot, the inflationary PMF scenario with axion strings is in tension with the astrophysical limit of  $f_a\gtrsim 10^8\,{\rm GeV}$  from supernova cooling [85].

### 6 Conclusion and Discussion

In this paper, we point out the comsmological implications of the chiral superconductivity of axion strings. The axion string network leaves a stable remnant, called the vorton, whose relic density depends on the efficiency of current leakage off the string. We have analytically estimated the vorton abundance today as a function of  $f_a$  and showed that its abundance exceeds the dark matter abundance today, unless y, the Yukawa coupling of KSVZ fermions to SM fermions is large. This calls for further scrutiny of the cosmological bounds on vortons, as they are an automatic byproduct of the axion string scenario.

In addition, we analyzed the evolution of the axion string network in the presence of a PMF within the analytic VOS model of string evolution. We found that the induced

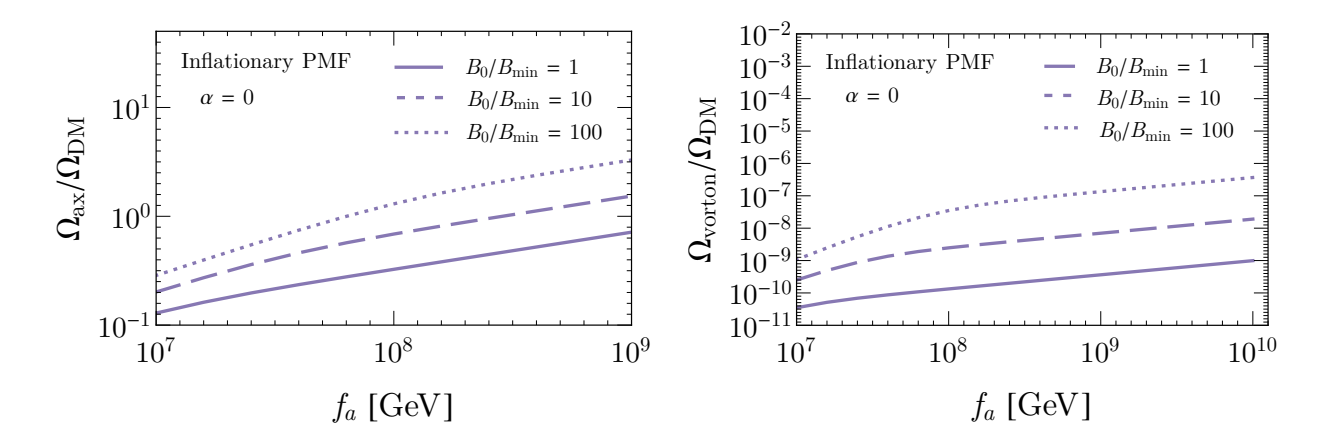


Figure 11. For the inflationary PMF, Left:  $\Omega_{\rm ax}/\Omega_{\rm DM}$ , Right:  $\Omega_{\rm v}/\Omega_{\rm DM}$  at  $T=1~{\rm GeV}$  as a function of  $f_a$  for a fixed  $T_{\rm init}$  and  $B_0$  today, scaled by the observed lower bound  $B_{\rm min} \equiv 3 \cdot 10^{-16} \,{\rm G}$ .  $f_a$  is taken to be  $10^{10} \,{\rm GeV}$ .

{fig:OmegaInF

current on the string is sizeable, creates a dominant friction force on the string, and suppresses string reconnections. This greatly increases the number of strings per Hubble volume, and eventually the relic axion abundance. We find that the inflationary PMF scenario, in combination with axion strings is disfavored for larger values of the magnetic field today, since the enhanced axion relic abundance implies  $f_a < 10^8 \,\text{GeV}$  in tension with astrophysical limits. For causal PMF generated by a first order phase transition in the early universe, our analysis implies an upper bound on the magnetogenesis temperature  $T_{\text{init}} \lesssim 100 \,\text{GeV}$ . We stress that our results have been obtained within the simplified VOS model for cosmic string evolution, and so need to be validated by future numerical studies.

# Acknowledgments

The authors would like to thank D. Arovas, J. Foster, M. Gorghetto, K. Kamada, K. Nakayama, T. Piran, B. Safdi, K. Saikawa, S. Shirai, and K. Yonekura, for useful discussions. HF and HM would like to thank J. Dror and J. Leedom for collaboration during the initial stage of this project. HF, HM and OT were supported by the Director, Office of Science, Office of High Energy Physics of the U.S. Department of Energy under the Contract No. DE-AC02-05CH11231, and AM under DOE Grant No. DE-SC0009919. The work of HM was also supported by the NSF grant PHY-1915314, by the JSPS Grant-in-Aid for Scientific Research JP17K05409, MEXT Grant-in-Aid for

Scientific Research on Innovative Areas JP15H05887, JP15K21733, by WPI, MEXT, Japan, and Hamamatsu Photonics, K.K..

## References

- [1] L. Ubaldi, Effects of theta on the deuteron binding energy and the triple-alpha process, Phys. Rev. D 81 (2010) 025011, [arXiv:0811.1599].
- [2] R. Peccei and H. R. Quinn, CP Conservation in the Presence of Instantons, Phys. Rev. Lett. 38 (1977) 1440–1443.
- [3] R. Peccei and H. R. Quinn, Constraints Imposed by CP Conservation in the Presence of Instantons, Phys. Rev. D 16 (1977) 1791–1797.
- [4] C. Vafa and E. Witten, Parity Conservation in QCD, Phys. Rev. Lett. 53 (1984) 535.
- [5] S. Weinberg, A New Light Boson?, Phys. Rev. Lett. 40 (1978) 223–226.
- [6] F. Wilczek, Problem of Strong P and T Invariance in the Presence of Instantons, Phys. Rev. Lett. 40 (1978) 279–282.
- [7] **Planck** Collaboration, N. Aghanim et al., *Planck 2018 results. VI. Cosmological parameters*, arXiv:1807.06209.
- [8] C. Hikage, M. Kawasaki, T. Sekiguchi, and T. Takahashi, Extended analysis of CMB constraints on non-Gaussianity in isocurvature perturbations, JCAP 03 (2013) 020, [arXiv:1212.6001].
- [9] T. Kobayashi, R. Kurematsu, and F. Takahashi, Isocurvature Constraints and Anharmonic Effects on QCD Axion Dark Matter, JCAP 09 (2013) 032, [arXiv:1304.0922].
- [10] T. Kibble, Some Implications of a Cosmological Phase Transition, Phys. Rept. 67 (1980) 183.
- [11] T. Kibble, Topology of Cosmic Domains and Strings, J. Phys. A 9 (1976) 1387–1398.
- [12] W. Zurek, Cosmological experiments in condensed matter systems, Phys. Rept. 276 (1996) 177–221, [cond-mat/9607135].
- [13] W. Zurek, Cosmological Experiments in Superfluid Helium?, Nature **317** (1985) 505–508.
- [14] H. Murayama and J. Shu, *Topological Dark Matter*, *Phys. Lett. B* **686** (2010) 162–165, [arXiv:0905.1720].
- [15] M. Nagasawa, Scaling distribution of axionic strings and estimation of axion density from axionic domain walls, Prog. Theor. Phys. **98** (1997) 851, [hep-ph/9712341].

- [16] D. P. Bennett and F. R. Bouchet, High resolution simulations of cosmic string evolution. 1. Network evolution, Phys. Rev. D 41 (1990) 2408.
- [17] B. Allen and E. Shellard, Cosmic string evolution: a numerical simulation, Phys. Rev. Lett. **64** (1990) 119–122.
- [18] V. Vanchurin, K. Olum, and A. Vilenkin, Cosmic string scaling in flat space, Phys. Rev. D 72 (2005) 063514, [gr-qc/0501040].
- [19] K. D. Olum and V. Vanchurin, Cosmic string loops in the expanding Universe, Phys. Rev. D 75 (2007) 063521, [astro-ph/0610419].
- [20] T. Hiramatsu, M. Kawasaki, T. Sekiguchi, M. Yamaguchi, and J. Yokoyama, Improved estimation of radiated axions from cosmological axionic strings, Phys. Rev. D 83 (2011) 123531, [arXiv:1012.5502].
- [21] J. J. Blanco-Pillado, K. D. Olum, and B. Shlaer, Large parallel cosmic string simulations: New results on loop production, Phys. Rev. D 83 (2011) 083514, [arXiv:1101.5173].
- [22] T. Hiramatsu, M. Kawasaki, K. Saikawa, and T. Sekiguchi, Production of dark matter axions from collapse of string-wall systems, Phys. Rev. D 85 (2012) 105020, [arXiv:1202.5851]. [Erratum: Phys.Rev.D 86, 089902 (2012)].
- [23] M. Kawasaki, K. Saikawa, and T. Sekiguchi, Axion dark matter from topological defects, Phys. Rev. D 91 (2015), no. 6 065014, [arXiv:1412.0789].
- [24] L. Fleury and G. D. Moore, Axion dark matter: strings and their cores, JCAP 01 (2016) 004, [arXiv:1509.00026].
- [25] V. B. Klaer and G. D. Moore, The dark-matter axion mass, JCAP 11 (2017) 049, [arXiv:1708.07521].
- [26] V. B. Klaer and G. D. Moore, How to simulate global cosmic strings with large string tension, JCAP 10 (2017) 043, [arXiv:1707.05566].
- [27] M. Gorghetto, E. Hardy, and G. Villadoro, Axions from Strings: the Attractive Solution, JHEP 07 (2018) 151, [arXiv:1806.04677].
- [28] A. Vaquero, J. Redondo, and J. Stadler, Early seeds of axion miniclusters, JCAP 04 (2019) 012, [arXiv:1809.09241].
- [29] M. Buschmann, J. W. Foster, and B. R. Safdi, Early-Universe Simulations of the Cosmological Axion, arXiv:1906.00967.
- [30] M. Hindmarsh, J. Lizarraga, A. Lopez-Eiguren, and J. Urrestilla, Scaling Density of Axion Strings, Phys. Rev. Lett. 124 (2020), no. 2 021301, [arXiv:1908.03522].
- [31] V. B. Klaer and G. D. Moore, Global cosmic string networks as a function of tension, arXiv:1912.08058.

- [32] K. Saikawa, "Axion dark matter mass: Towards a reliable estimate." http://research.ipmu.jp/seminar/sysimg/seminar/2360.pdf.
- [33] M. Gorghetto, E. Hardy, and G. Villadoro, *More Axions from Strings*, arXiv: 2007.04990.
- [34] J. E. Kim, Weak Interaction Singlet and Strong CP Invariance, Phys. Rev. Lett. 43 (1979) 103.
- [35] M. A. Shifman, A. Vainshtein, and V. I. Zakharov, Can Confinement Ensure Natural CP Invariance of Strong Interactions?, Nucl. Phys. B 166 (1980) 493–506.
- [36] C. G. Callan, Jr. and J. A. Harvey, Anomalies and Fermion Zero Modes on Strings and Domain Walls, Nucl. Phys. B250 (1985) 427–436.
- [37] R. Davis and E. Shellard, The Physics of Vortex Superconductivity. 2, Phys. Lett. B 209 (1988) 485–490.
- [38] B. Carter and X. Martin, Dynamic instability criterion for circular (Vorton) string loops, Annals Phys. 227 (1993) 151–171, [hep-th/0306111].
- [39] R. H. Brandenberger, B. Carter, A.-C. Davis, and M. Trodden, *Cosmic vortons and particle physics constraints*, *Phys. Rev. D* **54** (1996) 6059–6071, [hep-ph/9605382].
- [40] C. Martins and E. Shellard, Vorton formation, Phys. Rev. D 57 (1998) 7155–7176, [hep-ph/9804378].
- [41] C. Martins and E. Shellard, Limits on cosmic chiral vortons, Phys. Lett. B 445 (1998) 43–51, [hep-ph/9806480].
- [42] B. Carter and A.-C. Davis, *Chiral vortons and cosmological constraints on particle physics*, *Phys. Rev. D* **61** (2000) 123501, [hep-ph/9910560].
- [43] R. Jackiw and P. Rossi, Zero Modes of the Vortex Fermion System, Nucl. Phys. **B190** (1981) 681–691.
- [44] E. J. Weinberg, Index Calculations for the Fermion-Vortex System, Phys. Rev. D24 (1981) 2669.
- [45] J. Goldstone and F. Wilczek, Fractional Quantum Numbers on Solitons, Phys. Rev. Lett. 47 (1981) 986–989. [,365(1981); ,365(1981)].
- [46] D. B. Kaplan and A. Manohar, Anomalous Vortices and Electromagnetism, Nucl. Phys. B302 (1988) 280–290.
- [47] S. G. Naculich, Axionic Strings: Covariant Anomalies and Bosonization of Chiral Zero Modes, Nucl. Phys. B296 (1988) 837–867.
- [48] H. Fukuda and K. Yonekura, Witten effect, anomaly inflow, and charge teleportation, . In preparation.

- [49] A. Manohar, Anomalous Vortices and Electromagnetism. 2., Phys. Lett. B206 (1988) 276. [Erratum: Phys. Lett.209,543(1988)].
- [50] E. Witten, Superconducting Strings, Nucl. Phys. **B249** (1985) 557–592.
- [51] D. Harari and P. Sikivie, Effects of a Nambu-Goldstone boson on the polarization of radio galaxies and the cosmic microwave background, Phys. Lett. **B289** (1992) 67–72.
- [52] M. A. Fedderke, P. W. Graham, and S. Rajendran, Axion Dark Matter Detection with CMB Polarization, Phys. Rev. **D100** (2019), no. 1 015040, [arXiv:1903.02666].
- [53] A. Sen, Macroscopic charged heterotic string, Nucl. Phys. B 388 (1992) 457–473, [hep-th/9206016].
- [54] A. Davis, T. Kibble, M. Pickles, and D. A. Steer, Dynamics and properties of chiral cosmic strings in Minkowski space, Phys. Rev. D 62 (2000) 083516, [astro-ph/0005514].
- [55] T. Vachaspati and A. Vilenkin, Formation and Evolution of Cosmic Strings, Phys. Rev. D 30 (1984) 2036.
- [56] A. Vilenkin, Cosmic string dynamics with friction, Phys. Rev. D 43 (1991) 1060–1062.
- [57] E. Chudnovsky, G. Field, D. Spergel, and A. Vilenkin, Superconducting cosmic strings, Phys. Rev. D 34 (1986) 944–950.
- [58] K. Dimopoulos and A.-C. Davis, Friction domination with superconducting strings, Phys. Rev. D 57 (1998) 692–701, [hep-ph/9705302].
- [59] B. Carter, R. H. Brandenberger, A. Davis, and G. Sigl, Prolongation of friction dominated evolution for superconducting cosmic strings, JHEP 11 (2000) 019, [hep-ph/0009278].
- [60] A. Vilenkin and E. S. Shellard, Cosmic Strings and Other Topological Defects. Cambridge University Press, 7, 2000.
- [61] D. Gaiotto, Z. Komargodski, and N. Seiberg, *Time-reversal breaking in QCD*<sub>4</sub>, walls, and dualities in 2 + 1 dimensions, *JHEP* **01** (2018) 110, [arXiv:1708.06806].
- [62] Y. Hidaka, M. Nitta, and R. Yokokura, *Higher-form symmetries and 3-group in axion electrodynamics*, *Phys. Lett. B* **808** (2020) 135672, [arXiv:2006.12532].
- [63] J. S. Schwinger, On gauge invariance and vacuum polarization, Phys. Rev. 82 (1951) 664–679. [,116(1951)].
- [64] G. 't Hooft, Gauge Fields with Unified Weak, Electromagnetic, and Strong Interactions, in 1975 High-Energy Particle Physics Divisional Conference of EPS (includes 8th biennial conf on Elem. Particles), p. 1225, 9, 1975.
- [65] S. Mandelstam, Vortices and Quark Confinement in Nonabelian Gauge Theories, Phys. Rept. 23 (1976) 245–249.

- [66] V. De Luca, A. Mitridate, M. Redi, J. Smirnov, and A. Strumia, Colored Dark Matter, Phys. Rev. D 97 (2018), no. 11 115024, [arXiv:1801.01135].
- [67] R. Peccei, T. T. Wu, and T. Yanagida, A viable axion model, Phys. Lett. B 172 (1986) 435–440.
- [68] L. M. Krauss and F. Wilczek, A shortlived axion variant, Phys. Lett. B 173 (1986) 189–192.
- [69] E. N. Parker, Hydromagnetic Dynamo Models, Astrophys. J. 122 (1955) 293.
- [70] A. Neronov and I. Vovk, Evidence for strong extragalactic magnetic fields from Fermi observations of TeV blazars, Science 328 (2010) 73–75, [arXiv:1006.3504].
- [71] R. Durrer and A. Neronov, Cosmological Magnetic Fields: Their Generation, Evolution and Observation, Astron. Astrophys. Rev. 21 (2013) 62, [arXiv:1303.7121].
- [72] K. Subramanian, The origin, evolution and signatures of primordial magnetic fields, Rept. Prog. Phys. **79** (2016), no. 7 076901, [arXiv:1504.02311].
- [73] K. Jedamzik and A. Saveliev, Stringent Limit on Primordial Magnetic Fields from the Cosmic Microwave Background Radiation, Phys. Rev. Lett. 123 (2019), no. 2 021301, [arXiv:1804.06115].
- [74] C. Martins and E. Shellard, Quantitative string evolution, Phys. Rev. D 54 (1996) 2535–2556, [hep-ph/9602271].
- [75] R. Banerjee and K. Jedamzik, The Evolution of cosmic magnetic fields: From the very early universe, to recombination, to the present, Phys. Rev. D 70 (2004) 123003, [astro-ph/0410032].
- [76] V. Demozzi, V. Mukhanov, and H. Rubinstein, Magnetic fields from inflation?, JCAP 08 (2009) 025, [arXiv:0907.1030].
- [77] R. Durrer and C. Caprini, Primordial magnetic fields and causality, JCAP 11 (2003) 010, [astro-ph/0305059].
- [78] K. Kamada, Y. Tsai, and T. Vachaspati, Magnetic Field Transfer From A Hidden Sector, Phys. Rev. D 98 (2018) 043501, [arXiv:1803.08051].
- [79] A. C. Thompson, Cosmological Effects of Superconducting Strings, thesis, 10, 1988.
- [80] M. B. Mijic, Turning on a superconducting cosmic string, Phys. Rev. D 39 (1989) 2864.
- [81] C. Martins and E. Shellard, Extending the velocity dependent one scale string evolution model, Phys. Rev. D 65 (2002) 043514, [hep-ph/0003298].
- [82] J. Correia and C. Martins, Extending and Calibrating the Velocity dependent One-Scale model for Cosmic Strings with One Thousand Field Theory Simulations, Phys. Rev. D 100 (2019), no. 10 103517, [arXiv:1911.03163].

- [83] M. Yamaguchi, Cosmological evolution of cosmic strings with time dependent tension, Phys. Rev. D 72 (2005) 043533, [hep-ph/0503227].
- [84] C. Martins, Scaling properties of cosmological axion strings, Phys. Lett. B **788** (2019) 147–151, [arXiv:1811.12678].
- [85] **Particle Data Group** Collaboration, P. Zyla et al., *Review of Particle Physics*, *PTEP* **2020** (2020), no. 8 083C01.